

LU TP 17-19
June 2017

ABELIAN GAUGE SYMMETRIES IN THE TWO-HIGGS-DOUBLET MODEL

Franz Teichmann

Department of Astronomy and Theoretical Physics, Lund University

Master thesis supervised by Hugo Serôdio (Roman Pasechnik)



LUND
UNIVERSITY

For my father...

Abstract

The two-Higgs-doublet model is a promising extension of the Standard Model of particle physics, but it contains a large number of free parameters. With the intention to constrain this freedom, the model has been studied under different symmetries. In particular, a full classification of Abelian global symmetries has been presented in 2011. However, breaking global symmetries spontaneously leads to unobserved Goldstone bosons. This thesis, however, covers a study of the two-Higgs-doublet model under local gauge symmetries, where the origin of Goldstone bosons is avoided from the beginning. In order to do this, we examine the global symmetry classification from 2011 in the context of gauge anomalies, which provides an important criterion to investigate the consistency of a gauge theory. As our main results, we find a total of thirteen anomaly-free gauge models that are presented in detail. In addition, we perform a more in-depth study of the simplest gauge model we found and demonstrate its ability to provide physical observables in agreement with experimental data using the example of the CKM matrix.

Populärvetenskaplig sammanfattning

Die Entdeckung des Higgs-Teilchens im Jahr 2012 markiert einen weiteren Meilenstein in der Erfolgsgeschichte des Standardmodells der Teilchenphysik. Als einziges Elementarteilchen mit Spin Null ist es essentieller Bestandteil für die vollständige Erklärung der Teilchenmassen im Rahmen des sogenannten Higgs-Mechanismus.

Der experimentelle Nachweis dieses „Gottesteilchens“ ist nicht nur eine beeindruckende technische Leistung, sondern er eröffnet auch die Möglichkeit, das Standardmodell um zusätzliche Higgs-Felder zu erweitern. Die Beschränkung auf ein einzelnes Higgs-Feld ist zwar ökonomisch, jedoch nicht theoretisch fundiert.

Durch die Vielzahl an potentiellen Wechselwirkungen der zusätzlichen Higgs-Felder mit den Feldern des Standardmodells, weisen Multi-Higgs-Modelle eine hohe Anzahl an neuen Parametern auf, die fixiert werden müssen, um physikalische Vorhersagen treffen zu können.

Eine Möglichkeit zur Reduktion der Menge an freien Parametern ist das Auferlegen von Symmetrien, was nach dem sogenannten Noether-Theorem das Auftreten von Erhaltungsgrößen, also fixierten Parametern, herbeiführt.

In der vorliegenden Arbeit untersuchen wir die Erweiterung des Standardmodells um ein zweites Higgs-Feld, auch bekannt als 2-Higgs-Dublett-Modell, auf die Möglichkeit der Auferlegung einer abelschen Eichsymmetrie. Dabei liegt der Fokus auf der Vermeidung von Symmetrieverletzungen auf dem Quantenlevel, sogenannten Eichanomalien, welche die Konsistenz der zugrunde liegenden Eichtheorie zerstören würden.

Contents

1	Introduction	1
2	Theory part	3
2.1	Lie groups and generators	3
2.2	Noether's theorem and conserved currents	3
2.3	Abelian anomalies	4
2.3.1	Abelian currents	4
2.3.2	Abelian Ward identities	5
2.3.3	Anomalous Abelian Ward identities	6
2.4	Non-Abelian anomalies	11
2.4.1	Non-Abelian currents	11
2.4.2	Non-Abelian Ward identities	11
2.4.3	Anomalous non-Abelian Ward identities	12
2.5	Importance of Anomalies	14
2.6	Anomalies in the Standard Model of particle physics	14
2.6.1	Particle content and Electroweak Lagrangian of the Standard Model	14
2.6.2	Anomaly cancellation in the Standard Model	16
3	Abelian symmetries in the 2HDM	20
3.1	The two-Higgs-doublet model in more detail	20
3.1.1	Abelian global symmetries in the 2HDM quark sector	21
3.1.2	Finding physically relevant textures for the quark sector	22
3.2	Promoting the global symmetries to a gauge symmetries	23
3.2.1	Extended gauge group and anomaly equations	24
4	Implementation of anomaly cancellation into the 2HDM and resulting models	26
4.1	Quark sector only	26
4.1.1	Lagrangian and anomaly equations for the quark sector	26
4.1.2	Using textures as a starting point	27
4.1.3	Numerical procedure to rule out models	27
4.1.4	Categorisation of models via the number of different charges	31
4.1.5	Invariance under permutations	32
4.1.6	Possible models for the quark sector	33
4.1.7	Origin of the zero Higgs charge and extension to the lepton sector	34
4.2	Quarks and charged leptons	35
4.2.1	Anomaly equations for quarks and charged leptons	36
4.2.2	Numerical procedure for quarks and charged leptons	36
4.2.3	Possible models for quarks and charged leptons	38

5	Reproducing the CKM matrix for an example model	42
5.1	Down sector	42
5.2	Up sector	44
5.3	Parameter regions for a good CKM matrix	45
6	Conclusion and outlook	47
A	Appendix	49
A.1	Pauli matrices and Gell-Mann matrices	49
A.2	Dirac matrices	50
A.3	Time ordering	50
A.4	Shifting linear divergent integrals in Minkowski space	51
A.5	Feynman slash identities	51
A.6	Trivial anomaly cancellation	52
A.7	Goldstone's theorem	53

List of Figures

1	Contributing Feynman diagrams for $T^{\mu\nu\lambda}$	6
2	Contributing Feynman diagrams for $T^{\mu\nu}$	6
3	Contributing Feynman diagrams for $T_{abc}^{\mu\nu\lambda}$	12
4	Contributing Feynman diagrams for $T_{abc}^{\mu\nu}$	12
5	Decay $\pi^0(q) \rightarrow \gamma(k_1)\gamma(k_2)$ with $q = k_1 + k_2$	14
6	Triangle graph and generator assignment for the $[\text{SU}(3)]^2 \times \text{U}(1)$ anomaly.	17

List of Tables

1	SM particle content and representations under the gauge groups.	15
2	Particle content for $\text{SM} \times \text{U}(1)'$. $\text{U}(1)'$ charges are family-dependent.	24
3	Categorisation via number of different charges. Dark cells are forbidden, due to non-invertible mass matrices. Grey cells correspond to the categories covered by the textures in [9].	32
4	Categorisation of Table 3, highlighting the models that already allow for anomaly cancellation with quarks only (green cells).	33
5	Extension of Table 4 by the "quarks and charged leptons" models that allow for anomaly cancellation (blue cells). The latter feature always three different charges for l_i and e_i , respectively.	38

1 Introduction

The discovery of the Higgs boson at the LHC in 2012 [1], [2] represents a significant confirmation of one of the most experimentally tested and verified theories in modern particle physics: The Standard Model (SM hereafter). Due to its ability to provide reliable predictions of observables with high precision, it is considered one of the biggest achievements of theoretical physics of the last century.

However, despite its success, there are experimental facts that cannot be explained by the SM, for instance the lack of a viable dark matter candidate [3], the strong CP problem [4] or the hierarchy of quark masses [5]. Thus, a broad field of theoretical physics is devoted to what is known as physics beyond the SM (BSM).

The SM features three generations of fermions. With the first Higgs field experimentally confirmed, there is no theoretical reason to exclude the existence of multiple Higgs fields. Hence, there is a big interest in models with extended Higgs sectors [6]. The simplest one is the prominent two-Higgs-doublet model (2HDM hereafter), where the SM particle content is extended by a second scalar Higgs field. It provides options for spontaneous CP violation, baryogenesis, dark matter candidates as well as a solution to the strong CP problem [7].

A common downside of all multi-Higgs models is the large number of parameters that need to be fixed in order to make predictions. Thankfully, it is possible to reduce the number of free parameters by imposing symmetries on the model, which lead to conserved quantities, as stated in the famous Noether's theorem [8].

In the case of Abelian symmetries, a full study and classification of physical models for the quark sector has been done by Ferreira and Silva in 2011 [9]. Starting from imposing the most general case of a global flavour-dependent symmetry, the resulting Yukawa textures were derived and presented for discrete and continuous symmetries, respectively.

In conformity with the SM, the 2HDM relies on spontaneous symmetry breaking as the mechanism to provide masses for the gauge bosons. Having said this, the restriction of parameters via a continuous global symmetry is problematic, because when spontaneously broken, a new massless scalar particle appears [10]. However, these so-called Goldstone bosons have not been observed experimentally.

One possible solution that avoids the appearance of Goldstone bosons is the restriction of parameters via local symmetries in the framework of gauge theory [4]. Unfortunately, the consistency of a gauge theory may be spoiled by quantum corrections to the symmetry, known as gauge anomalies [11]. Thus, any coherent gauge theory has to be free of anomalies.

In this thesis, we will examine the models presented by [9] in the context of anomalies and investigate if some of the initially global symmetries can be promoted to gauge symmetries.

The thesis is organised as follows: Section 2 provides the theoretical background needed

for the understanding of anomalies. We present a full derivation of their origin, as well as a discussion of the importance of anomalies in the context of the SM.

Throughout section 3, we present the 2HDM in more detail and discuss how the constrained models were derived from the global Abelian symmetries in [9]. After emphasising the necessity for gauge symmetries, we present how the models are examined in the context of anomalies and derive the relevant system of equations that ensures anomaly cancellation.

Section 4 expands on how the cancellation of anomalies is implemented numerically and represents the main section of the thesis. It is divided into two parts: In the first part, we present the technicalities and results for a study of the quark sector. In the second part, the studies are extended to include the lepton sector and more results are presented.

In section 5, we perform a more in-depth study on one of the presented (anomaly-free) models. We demonstrate its ability to reproduce the CKM matrix as an illustration of the physical applicability of the models presented in this thesis.

Finally, conclusion and outlook are presented in section 6.

2 Theory part

2.1 Lie groups and generators

The most relevant groups in physics are *Lie groups*. Throughout this thesis, the relevant groups are simple Lie groups, which are characterised by the fact that all elements are continuously connected to the identity element via

$$g(x) = e^{-i\Lambda(x)} \quad \text{with} \quad \Lambda(x) = \Lambda^a(x)T^a. \quad (2.1)$$

So there is a set of operators T^a which determine the structure of the Lie group and numbers $\Lambda^a(x)$ that parametrise the different group elements.¹ The T^a are called *group generators*. They form a Lie algebra, which means they satisfy the commutation relations

$$[T^a, T^b] = if^{abc}T^c, \quad (2.2)$$

where the totally antisymmetric f^{abc} are numbers called structure constants [12]. If all generators commute, that means all $f^{abc} \equiv 0$, the Lie group is said to be Abelian. Otherwise, it is called non-Abelian.²

For our purposes, the Abelian group of interest is $U(1)$, with the generator $T_{U(1)} = 1$. In addition, there are two non-Abelian groups of importance, namely $SU(2)$ and $SU(3)$. Their generators are given as

$$T_{SU(2)}^j = \frac{\sigma^j}{2} \quad \text{and} \quad T_{SU(3)}^a = \frac{\lambda^a}{2} \quad (2.3)$$

respectively, where σ^j label the Pauli matrices and λ^a are the Gell-Mann matrices (for more details see A.1). This means that their generators are all Hermitian

$$T_{SU(2)}^{j\dagger} = T_{SU(2)}^j, \quad T_{SU(3)}^{a\dagger} = T_{SU(3)}^a \quad (2.4)$$

and traceless

$$\text{Tr} \left(T_{SU(2)}^j \right) \propto \text{Tr} (\sigma^j) \equiv 0, \quad \text{Tr} \left(T_{SU(3)}^a \right) \propto \text{Tr} (\lambda^a) \equiv 0. \quad (2.5)$$

2.2 Noether's theorem and conserved currents

In Lagrangian field theory we have the Lagrangian density $\mathcal{L}(\phi, \partial_\mu \phi)$ that contains the information about our system. To be more precise, taking the integral over four dimensions (three spatial and one time component) gives the relevant quantity S , called "action".

$$S = \int \mathcal{L}(\phi_a, \partial_\mu \phi_a) d^4x \quad (2.6)$$

¹The space-time dependence is not relevant for the general discussion of Lie groups, but will come into play when we look at Lie groups in the context of gauge groups later.

²We will also encounter products of simple Lie groups, referred to as semisimple Lie groups. Their elements are still continuously connected and the discussion of this section holds.

The so-called "principle of least action" states that a system in a given state evolves to another state along the path of minimal action [10]. This leads to the Euler-Lagrange equations of motion:

$$\partial_\mu \left(\frac{\partial \mathcal{L}}{\partial(\partial_\mu \phi_a)} \right) = \frac{\partial \mathcal{L}}{\partial \phi_a} \quad (2.7)$$

In classical field theory, every continuous symmetry of a system corresponds to a conserved quantity, usually called current - a fact that is summarised in *Noether's theorem*. The idea is to look at the infinitesimal case of the symmetry transformation on the fields

$$\phi_a(x) \rightarrow \phi'_a(x) = \phi_a(x) + \varepsilon \Delta \phi_a(x), \quad (2.8)$$

where the deformations of the fields $\Delta \phi_a$ under the given transformation are regulated by the infinitesimal parameter ε .³ For the equations of motion to hold (symmetry!), the Lagrangian must be invariant up to a 4-divergence, which can be written as

$$\varepsilon \Delta \mathcal{L}(x) = \mathcal{L}'(x) - \mathcal{L}(x) \stackrel{!}{=} \varepsilon \partial_\mu \mathcal{J}^\mu(x), \quad (2.9)$$

with $\mathcal{J}^\mu(x)$ being some function. On the other hand, the shift in the Lagrangian under the symmetry transformation is given by

$$\begin{aligned} \varepsilon \Delta \mathcal{L} &= \frac{\partial \mathcal{L}}{\partial \phi_a} (\varepsilon \Delta \phi_a) + \left(\frac{\partial \mathcal{L}}{\partial(\partial_\mu \phi_a)} \right) \partial_\mu (\varepsilon \Delta \phi_a) \\ &= \varepsilon \partial_\mu \left(\frac{\partial \mathcal{L}}{\partial(\partial_\mu \phi_a)} \Delta \phi_a \right) + \varepsilon \underbrace{\left[\frac{\partial \mathcal{L}}{\partial \phi_a} - \partial_\mu \left(\frac{\partial \mathcal{L}}{\partial(\partial_\mu \phi_a)} \right) \right]}_{=0} \Delta \phi_a, \end{aligned} \quad (2.10)$$

where the second term vanishes due to the equations of motion (2.7). Hence, by combining (2.9) and (2.10), one finds that there is a *conserved current*

$$j^\mu(x) = \frac{\partial \mathcal{L}}{\partial(\partial_\mu \phi_a)}(x) \Delta \phi_a(x) - \mathcal{J}^\mu(x) \quad \text{for which} \quad \partial_\mu j^\mu(x) = 0. \quad (2.11)$$

2.3 Abelian anomalies

2.3.1 Abelian currents

In order to find the Abelian currents, consider the QED Lagrangian as an example. Using the standard Feynman slash notation $\not{a} := \gamma^\mu a_\mu$ with γ^μ denoting the Dirac matrices (see appendix A.2), it can be written as

$$\mathcal{L}_{\text{QED}} = \bar{\psi}(i\not{\partial} - m + e\not{A})\psi - \frac{1}{4}F_{\mu\nu}F^{\mu\nu} \quad \text{with} \quad F_{\mu\nu} = \partial_\mu A_\nu - \partial_\nu A_\mu, \quad (2.12)$$

³ $\Delta \phi_a$ denotes the full change under the symmetry, composed of the change in fields and the change in coordinates. Thus, this discussion is not limited to internal symmetries.

where A_μ is the Abelian gauge field and the coupling is labelled as e . Amongst others, it is now possible to construct the following currents:

$$\text{vector} \qquad j^\mu = \bar{\psi}\gamma^\mu\psi \qquad (2.13)$$

$$\text{axial} \qquad j_5^\mu = \bar{\psi}\gamma^\mu\gamma^5\psi \qquad (2.14)$$

$$\text{pseudoscalar} \qquad P = \bar{\psi}\gamma^5\psi \qquad (2.15)$$

Using the equations of motion (2.7) and the Lagrangian (2.12), it can be checked that

$$\partial_\mu j^\mu = 0 \quad \text{and} \quad \partial_\mu j_5^\mu = 2imP, \qquad (2.16)$$

so the vector current is indeed conserved; same is true for the axial current in the case of massless fermions, i.e. $m = 0$ [11].

2.3.2 Abelian Ward identities

In particle physics, we are dealing with quantised energy, giving rise to quantum fields. Therefore, we have to find an equivalent to the classical conservation laws (2.16) in quantum field theory, known as Ward identities.

Considering the derivate of the time ordered product, denoted by the time ordering operator \mathcal{T} (see appendix A.3), of a current $j^\mu(x)$ and an operator $\hat{O}(y)$ yields the identity

$$\partial_\mu^x \left(\mathcal{T} j^\mu(x) \hat{O}(y) \right) = \mathcal{T} \partial_\mu^x j^\mu(x) \hat{O}(y) + \left[j^0(x), \hat{O}(y) \right] \delta(x_0 - y_0), \qquad (2.17)$$

where $\delta(x)$ labels the one-dimensional Dirac delta function. The last term is known as Schwinger term [13]. The above identity allows one to study the 3-point functions

$$\langle 0 | \mathcal{T} j^\mu(x) j^\nu(y) j_5^\lambda(z) | 0 \rangle \quad \text{and} \quad \langle 0 | \mathcal{T} j^\mu(x) j^\nu(y) P(z) | 0 \rangle \qquad (2.18)$$

in momentum space. Defining the amplitudes

$$T^{\mu\nu\lambda}(k_1, k_2, q) := i \int d^4x d^4y d^4z e^{ik_1x + ik_2y - iqz} \langle 0 | \mathcal{T} j^\mu(x) j^\nu(y) j_5^\lambda(z) | 0 \rangle \qquad (2.19)$$

$$T^{\mu\nu}(k_1, k_2, q) := i \int d^4x d^4y d^4z e^{ik_1x + ik_2y - iqz} \langle 0 | \mathcal{T} j^\mu(x) j^\nu(y) P(z) | 0 \rangle, \qquad (2.20)$$

it can be found by partial integration that, up to a surface term,

$$q_\lambda T^{\mu\nu\lambda} = - \int d^4x d^4y d^4z \partial_\lambda^z \left(e^{ik_1x + ik_2y - iqz} \right) \langle 0 | \mathcal{T} j^\mu(x) j^\nu(y) j_5^\lambda(z) | 0 \rangle \qquad (2.21)$$

$$= \int d^4x d^4y d^4z e^{ik_1x + ik_2y - iqz} \partial_\lambda^z \left(\langle 0 | \mathcal{T} j^\mu(x) j^\nu(y) j_5^\lambda(z) | 0 \rangle \right) \qquad (2.22)$$

$$= \int d^4x d^4y d^4z e^{ik_1x + ik_2y - iqz} \langle 0 | \mathcal{T} j^\mu(x) j^\nu(y) \partial_\lambda^z j_5^\lambda(z) | 0 \rangle + \text{Schwinger term}, \qquad (2.23)$$

where (2.17) was used in the last step. Neglecting the Schwinger term (for a discussion see [14]) and using the classical conservation laws from (2.16), it follows that

$$q_\lambda T^{\mu\nu\lambda} = 2mi \int d^4x d^4y d^4z e^{ik_1x+ik_2y-iqz} \langle 0 | \mathcal{T} j^\mu(x) j^\nu(y) P(z) | 0 \rangle = 2mT^{\mu\nu}. \quad (2.24)$$

This relation is known as *axial Ward identity*. Analogously, it can be checked that, up to Schwinger terms, the following *vector Ward identities* hold [11]:

$$\begin{aligned} k_{1\mu} T^{\mu\nu\lambda} &= - \int d^4x d^4y d^4z e^{ik_1x+ik_2y-iqz} \langle 0 | \mathcal{T} \underbrace{\partial_\mu^x j^\mu(x)}_{=0} j^\nu(y) j_5^\lambda(z) | 0 \rangle = 0 \\ k_{2\nu} T^{\mu\nu\lambda} &= - \int d^4x d^4y d^4z e^{ik_1x+ik_2y-iqz} \langle 0 | \mathcal{T} j^\mu(x) \underbrace{\partial_\nu^y j^\nu(y)}_{=0} j_5^\lambda(z) | 0 \rangle = 0 \end{aligned} \quad (2.25)$$

2.3.3 Anomalous Abelian Ward identities

In this section, the Abelian Ward identities, as introduced in (2.24) and (2.25), will be recalculated directly by the use of Feynman rules. It will turn out that there are unavoidable corrections, which means that the currents are not conserved at quantum level. This phenomenon is called an *anomaly*. The derivation presented here follows the logic of [11].

The amplitudes defined in (2.19) and (2.20) correspond to the Feynman diagrams shown in Figure 1 and Figure 2, respectively [15]:

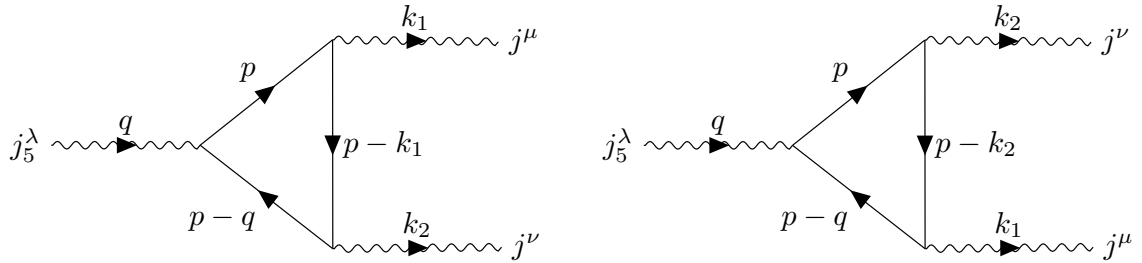


Figure 1: Contributing Feynman diagrams for $T^{\mu\nu\lambda}$.

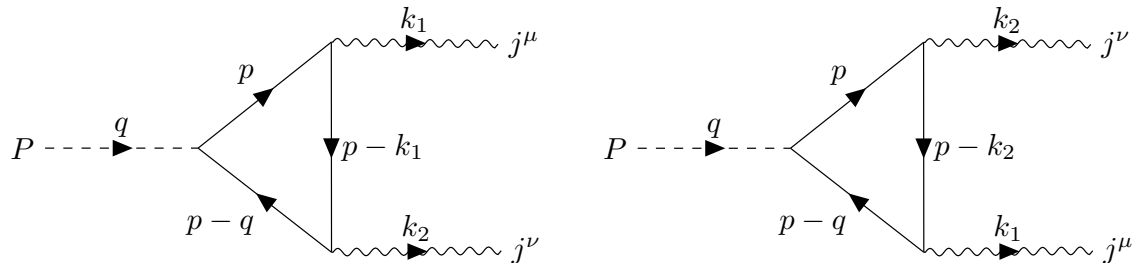


Figure 2: Contributing Feynman diagrams for $T^{\mu\nu}$.

Using Feynman rules (a nice summary can be found in [3]), one finds

$$T^{\mu\nu\lambda} = -i \int \frac{d^4p}{(2\pi)^4} \text{Tr} \left(\frac{i}{\not{p} - m} \gamma^\lambda \gamma^5 \frac{i}{\not{p} - \not{q} - m} \gamma^\nu \frac{i}{\not{p} - \not{k}_1 - m} \gamma^\mu \right) + \left(\begin{array}{c} k_1 \leftrightarrow k_2 \\ \mu \leftrightarrow \nu \end{array} \right) \quad (2.26)$$

as well as

$$T^{\mu\nu} = -i \int \frac{d^4p}{(2\pi)^4} \text{Tr} \left(\frac{i}{\not{p} - m} \gamma^5 \frac{i}{\not{p} - \not{q} - m} \gamma^\nu \frac{i}{\not{p} - \not{k}_1 - m} \gamma^\mu \right) + \left(\begin{array}{c} k_1 \leftrightarrow k_2 \\ \mu \leftrightarrow \nu \end{array} \right), \quad (2.27)$$

where $q = k_1 + k_2$ ensures momentum conservation.

2.3.3.1 Anomalous axial Ward identity

The axial Ward identity is recalculated by substituting the slash identity (A.20) into (2.26). Given (2.27), the substitution yields

$$q_\lambda T^{\mu\nu\lambda} = 2mT^{\mu\nu} + R^{\mu\nu}, \quad (2.28)$$

which differs from (2.24) by a correction term

$$R^{\mu\nu} = \int \frac{d^4p}{(2\pi)^4} \text{Tr} \left(\frac{1}{\not{p} - \not{k}_1 - m} \gamma^5 \gamma^\mu \frac{1}{\not{p} - \not{q} - m} \gamma^\nu - \frac{1}{\not{p} - m} \gamma^5 \gamma^\mu \frac{1}{\not{p} - \not{k}_2 - m} \gamma^\nu \right) + \left(\begin{array}{c} k_1 \leftrightarrow k_2 \\ \mu \leftrightarrow \nu \end{array} \right). \quad (2.29)$$

Since $q = k_1 + k_2$, the correction term can be rewritten in a more compact form [13]:

$$R^{\mu\nu} = \int \frac{d^4p}{(2\pi)^4} \left[f^{\mu\nu}(p - k_1, k_2) - f^{\mu\nu}(p, k_2) + \left(\begin{array}{c} k_1 \leftrightarrow k_2 \\ \mu \leftrightarrow \nu \end{array} \right) \right], \quad (2.30)$$

where

$$f^{\mu\nu}(p, k) := \text{Tr} \left(\frac{1}{\not{p} - m} \gamma^5 \gamma^\mu \frac{1}{\not{p} - \not{k} - m} \gamma^\nu \right). \quad (2.31)$$

In this notation, it can be seen that the correction term arises from a shift in the integration variable, due to the linear divergence of the integral. Using the result from appendix A.4, it follows that

$$R^{\mu\nu} = i2\pi^2(-k_{1\lambda}) \lim_{p \rightarrow \infty} p^\lambda p^2 \frac{\text{Tr} \left((\not{p} + m) \gamma^5 \gamma^\mu (\not{p} - \not{k}_2 + m) \gamma^\nu \right)}{(2\pi)^4 [p^2 - m^2] [(p - k_2)^2 - m^2]} + \left(\begin{array}{c} k_1 \leftrightarrow k_2 \\ \mu \leftrightarrow \nu \end{array} \right) \quad (2.32)$$

$$= \frac{i}{8\pi^2}(-k_{1\lambda}) \lim_{p \rightarrow \infty} p^\lambda \frac{p_\rho (p - k_2)_\sigma}{p^2} \underbrace{\text{Tr} \left(\gamma^\rho \gamma^5 \gamma^\mu \gamma^\sigma \gamma^\nu \right)}_{=-4i\epsilon^{\rho\mu\sigma\nu}} + \left(\begin{array}{c} k_1 \leftrightarrow k_2 \\ \mu \leftrightarrow \nu \end{array} \right), \quad (2.33)$$

where the trace identity from A.2 is being used. Due to the antisymmetry of the Levi-Civita symbol ($p_\rho p_\sigma \varepsilon^{\rho\mu\sigma\nu} = 0$), the correction term reduces to

$$R^{\mu\nu} = \frac{1}{2\pi^2} \varepsilon^{\rho\mu\sigma\nu} k_{1\lambda} k_{2\sigma} \lim_{p \rightarrow \infty} \frac{p^\lambda p_\rho}{p^2} + \begin{pmatrix} k_1 \leftrightarrow k_2 \\ \mu \leftrightarrow \nu \end{pmatrix}. \quad (2.34)$$

The symmetric momentum limit (also discussed in [10])

$$\lim_{p \rightarrow \infty} \frac{p_\lambda p_\rho}{p^2} = \frac{g_{\lambda\rho}}{4} \quad (2.35)$$

yields the result

$$R^{\mu\nu} = \frac{1}{8\pi^2} \varepsilon^{\rho\mu\sigma\nu} k_{1\rho} k_{2\sigma} + \begin{pmatrix} k_1 \leftrightarrow k_2 \\ \mu \leftrightarrow \nu \end{pmatrix} = -\frac{1}{4\pi^2} \varepsilon^{\mu\nu\rho\sigma} k_{1\rho} k_{2\sigma}, \quad (2.36)$$

where the minus in the last step arises from the index exchange in the Levi-Civita symbol. Therefore, (2.28) takes the form

$$q_\lambda T^{\mu\nu\lambda} = 2mT^{\mu\nu} - \frac{1}{4\pi^2} \varepsilon^{\mu\nu\rho\sigma} k_{1\rho} k_{2\sigma}. \quad (2.37)$$

However, this is not the final result yet. Ambiguity remains in the amplitude $T^{\mu\nu\lambda}$, because the choice of the internal loop momentum p is not unique (see Figure 1). Since the integral in (2.26) is again linearly divergent, we can use the same procedure as for the correction term.⁴

Consider a class of loop momentum shifts $p \rightarrow p + a_i$ with

$$a_1 = \alpha(k_1 + k_2) - \beta k_2 \quad \text{and} \quad a_2 = \alpha(k_1 + k_2) - \beta k_1 \quad (2.38)$$

for the first and second diagram in Figure 1 respectively, parametrised by real numbers α and β . Please note that the two shifts differ only by the interchange $k_1 \leftrightarrow k_2$, which matches exactly the difference between the corresponding diagrams and hence is necessary in order to respect the Bose symmetry.

This class of shifts leads to a class of amplitude differences

$$\Delta^{\mu\nu\lambda}(\alpha, \beta) := T^{\mu\nu\lambda}(\alpha, \beta) - T^{\mu\nu\lambda}(0, 0) \quad (2.39)$$

$$= \int \frac{d^4 p}{(2\pi)^4} \left[f^{\mu\nu\lambda}(p + a_2, q, k_2) - f^{\mu\nu\lambda}(p, q, k_2) + \begin{pmatrix} k_1 \leftrightarrow k_2 \\ \mu \leftrightarrow \nu \end{pmatrix} \right], \quad (2.40)$$

where

$$f^{\mu\nu\lambda}(p, q, k) := \text{Tr} \left(\frac{1}{\not{p} - m} \gamma^5 \gamma^\lambda \frac{1}{\not{p} - \not{q} - m} \gamma^\mu \frac{1}{\not{p} - \not{k} - m} \gamma^\nu \right). \quad (2.41)$$

⁴The amplitude $T^{\mu\nu}$ is unaffected by such a momentum shift, because the integral in (2.27) is convergent.

In this notation, it is evident that the above integral has a similar form as (2.31). Consequently, one finds

$$\Delta^{\mu\nu\lambda}(\alpha, \beta) = i2\pi^2 a_{2\xi} \lim_{p \rightarrow \infty} p^\xi p^2 \frac{\text{Tr} \left((\not{p} + m) \gamma^5 \gamma^\lambda (\not{p} - \not{q} + m) \gamma^\mu (\not{p} - \not{k}_2 + m) \gamma^\nu \right)}{(2\pi)^4 [p^2 - m^2] [(p - q)^2 - m^2] [(p - k_2)^2 - m^2]} + \left(\begin{array}{l} k_1 \leftrightarrow k_2 \\ \mu \leftrightarrow \nu \end{array} \right) \quad (2.42)$$

$$= \frac{i}{8\pi^2} a_{2\xi} \lim_{p \rightarrow \infty} \frac{p^\xi p_\rho (p - q)_\sigma (p - k_2)_\tau \text{Tr} \left(\gamma^\rho \gamma^5 \gamma^\lambda \gamma^\sigma \gamma^\mu \gamma^\tau \gamma^\nu \right)}{p^4} + \left(\begin{array}{l} k_1 \leftrightarrow k_2 \\ \mu \leftrightarrow \nu \end{array} \right) \quad (2.43)$$

$$= \frac{i}{8\pi^2} a_{2\xi} \lim_{p \rightarrow \infty} \frac{p^\xi p_\rho p_\sigma p_\tau \text{Tr} \left(\gamma^5 \gamma^\lambda \gamma^\sigma \gamma^\mu \gamma^\tau \gamma^\nu \gamma^\rho \right)}{p^4} + \left(\begin{array}{l} k_1 \leftrightarrow k_2 \\ \mu \leftrightarrow \nu \end{array} \right) \quad (2.44)$$

$$= \frac{i}{8\pi^2} a_{2\xi} \lim_{p \rightarrow \infty} \frac{p^\xi p_\sigma}{p^2} (-4i\varepsilon^{\lambda\sigma\mu\nu}) + \left(\begin{array}{l} k_1 \leftrightarrow k_2 \\ \mu \leftrightarrow \nu \end{array} \right), \quad (2.45)$$

where the trace identity from appendix A.2 was used. Applying, once again, the symmetric momentum limit (2.35) and substituting the expression for the shift a_2 (2.38) leads to

$$\Delta^{\mu\nu\lambda}(\alpha, \beta) = \frac{1}{8\pi^2} a_{2\sigma} \varepsilon^{\mu\nu\lambda\sigma} + \left(\begin{array}{l} k_1 \leftrightarrow k_2 \\ \mu \leftrightarrow \nu \end{array} \right) \quad (2.46)$$

$$= \frac{1}{8\pi^2} [\alpha(k_1 + k_2) - \beta k_1]_\sigma \varepsilon^{\mu\nu\lambda\sigma} + \left(\begin{array}{l} k_1 \leftrightarrow k_2 \\ \mu \leftrightarrow \nu \end{array} \right) \quad (2.47)$$

$$= -\frac{\beta}{8\pi^2} \varepsilon^{\mu\nu\lambda\sigma} (k_1 - k_2)_\sigma. \quad (2.48)$$

It is evident that the above result is independent of α . Consequently, β is the only relevant parameter for the shift. Combining (2.37), (2.39) and (2.48) yields

$$q_\lambda T^{\mu\nu\lambda}(\beta) = 2mT^{\mu\nu} - \frac{1}{4\pi^2} \varepsilon^{\mu\nu\rho\sigma} k_{1\rho} k_{2\sigma} - \frac{\beta}{8\pi^2} \varepsilon^{\mu\nu\lambda\sigma} \underbrace{(k_1 + k_2)_\lambda}_{=q_\lambda} (k_1 - k_2)_\sigma. \quad (2.49)$$

Because of $\varepsilon^{\mu\nu\rho\sigma} k_{1\rho} k_{1\sigma} = \varepsilon^{\mu\nu\rho\sigma} k_{2\rho} k_{2\sigma} = 0$, the last term may be reduced, thus providing the final result known as the *anomalous axial Ward identity*:

$$q_\lambda T^{\mu\nu\lambda}(\beta) = 2mT^{\mu\nu} - \frac{1 - \beta}{4\pi^2} \varepsilon^{\mu\nu\rho\sigma} k_{1\rho} k_{2\sigma} \quad (2.50)$$

2.3.3.2 Anomalous vector Ward identities

In a similar way, one may study the vector Ward identities. Starting from (2.26), one can apply the slash identities (A.21) to find

$$k_{1\mu}T^{\mu\nu\lambda} = \int \frac{d^4p}{(2\pi)^4} \left[\text{Tr} \left(\frac{1}{\not{p}-m} \gamma^5 \gamma^\lambda \frac{1}{\not{p}-\not{q}-m} \gamma^\nu \frac{1}{\not{p}-\not{k}_1-m} \not{k}_1 \right) + \text{Tr} \left(\frac{1}{\not{p}-m} \gamma^5 \gamma^\lambda \frac{1}{\not{p}-\not{q}-m} \not{k}_1 \frac{1}{\not{p}-\not{k}_2-m} \gamma^\nu \right) \right] \quad (2.51)$$

$$= \int \frac{d^4p}{(2\pi)^4} \left[\text{Tr} \left(\gamma^5 \gamma^\lambda \frac{1}{\not{p}-\not{q}-m} \gamma^\nu \frac{1}{\not{p}-\not{k}_1-m} \right) - \text{Tr} \left(\gamma^5 \gamma^\lambda \frac{1}{\not{p}-\not{k}_2-m} \gamma^\nu \frac{1}{\not{p}-m} \right) \right] \quad (2.52)$$

$$= \int \frac{d^4p}{(2\pi)^4} [f^{\lambda\nu}(p-k_1, k_2) - f^{\lambda\nu}(p, k_2)], \quad (2.53)$$

with the definition (2.31). This integral is identical to the first part of (2.30). Hence one can directly use the result given in (2.36):

$$k_{1\mu}T^{\mu\nu\lambda}(0) = \frac{1}{8\pi^2} \varepsilon^{\rho\lambda\sigma\nu} k_{1\rho} k_{2\sigma} = \frac{1}{8\pi^2} \varepsilon^{\nu\lambda\rho\sigma} k_{1\rho} k_{2\sigma} \quad (2.54)$$

The zero indicates that the amplitude is not shifted yet. This is taken care of by substituting (2.39) and using result (2.48):

$$k_{1\mu}T^{\mu\nu\lambda}(\beta) = \frac{1}{8\pi^2} \varepsilon^{\nu\lambda\rho\sigma} k_{1\rho} k_{2\sigma} - \frac{\beta}{8\pi^2} \varepsilon^{\mu\nu\lambda\sigma} k_{1\mu} (k_1 - k_2)_\sigma \quad (2.55)$$

From that, one finds the *anomalous vector Ward identities*, given as

$$k_{1\mu}T^{\mu\nu\lambda}(\beta) = \frac{1+\beta}{8\pi^2} \varepsilon^{\nu\lambda\rho\sigma} k_{1\rho} k_{2\sigma} \quad (2.56)$$

$$k_{2\nu}T^{\mu\nu\lambda}(\beta) = -\frac{1+\beta}{8\pi^2} \varepsilon^{\mu\lambda\rho\sigma} k_{1\rho} k_{2\sigma}.$$

2.3.3.3 Summary

A comparison between the Ward identities given in (2.24) and (2.25),

$$q_\lambda T^{\mu\nu\lambda} = 2mT^{\mu\nu} \quad \text{and} \quad \begin{aligned} k_{1\mu}T^{\mu\nu\lambda} &= 0 \\ k_{2\nu}T^{\mu\nu\lambda} &= 0, \end{aligned} \quad (2.57)$$

and the relations found directly using Feynman rules, (2.50) and (2.56),

$$q_\lambda T^{\mu\nu\lambda}(\beta) = 2mT^{\mu\nu} - \frac{1-\beta}{4\pi^2} \varepsilon^{\mu\nu\rho\sigma} k_{1\rho} k_{2\sigma} \quad \text{and} \quad \begin{aligned} k_{1\mu}T^{\mu\nu\lambda}(\beta) &= \frac{1+\beta}{8\pi^2} \varepsilon^{\nu\lambda\rho\sigma} k_{1\rho} k_{2\sigma} \\ k_{2\nu}T^{\mu\nu\lambda}(\beta) &= -\frac{1+\beta}{8\pi^2} \varepsilon^{\mu\lambda\rho\sigma} k_{1\rho} k_{2\sigma}, \end{aligned} \quad (2.58)$$

reveals that there are correction terms, parametrised by β . More importantly, it is evident that there is no possible choice of β , allowing for both Ward identities to be satisfied at the same time. So the anomaly remains for all possible shifts.

Choosing only the axial Ward identity to be anomalous, which means $\beta = -1$, yields

$$q_\lambda T^{\mu\nu\lambda} = 2mT^{\mu\nu} + \mathcal{A}^{\mu\nu} \quad \text{and} \quad k_{1\mu} T^{\mu\nu\lambda} = k_{2\nu} T^{\mu\nu\lambda} = 0, \quad (2.59)$$

with the famous Adler-Bell-Jackiw (ABJ hereafter) anomaly [16], [17] in momentum space

$$\mathcal{A}^{\mu\nu} = -\frac{1}{2\pi^2} \varepsilon^{\mu\nu\rho\sigma} k_{1\rho} k_{2\sigma}. \quad (2.60)$$

2.4 Non-Abelian anomalies

2.4.1 Non-Abelian currents

As an example for the non-Abelian case, consider the Lagrangian

$$\mathcal{L}_{\text{non-Abelian}} = \bar{\psi}(i\not{D} - m)\psi \quad \text{with} \quad D_\mu = \partial_\mu + ig_N N_\mu, \quad (2.61)$$

where $N_\mu = N_\mu^a T^a$ is a non-Abelian field and the coupling is denoted by g_N . In a similar way as in section 2.3.1, the following currents can be constructed:

$$\text{vector} \quad j_a^\mu = \bar{\psi} \gamma^\mu T^a \psi \quad (2.62)$$

$$\text{axial} \quad j_{5a}^\mu = \bar{\psi} \gamma^\mu \gamma^5 T^a \psi \quad (2.63)$$

$$\text{pseudoscalar} \quad P_a = \bar{\psi} \gamma^5 T^a \psi \quad (2.64)$$

The current conservation for the non-Abelian case has to be checked via the covariant derivative given in (2.61), which yields

$$D_\mu j_a^\mu = 0 \quad \text{and} \quad D_\mu j_{5a}^\mu = 2imP_a. \quad (2.65)$$

Thus, the vector current is covariantly conserved; as in the Abelian case, also the axial current is conserved for $m = 0$.⁵

2.4.2 Non-Abelian Ward identities

Analogously to (2.19) and (2.20), defining the amplitudes

$$T_{abc}^{\mu\nu\lambda}(k_1, k_2, q) := i \int d^4x d^4y d^4z e^{ik_1x + ik_2y - iqz} \langle 0 | \mathcal{T} j_a^\mu(x) j_b^\nu(y) j_{5c}^\lambda(z) | 0 \rangle \quad (2.66)$$

$$T_{abc}^{\mu\nu}(k_1, k_2, q) := i \int d^4x d^4y d^4z e^{ik_1x + ik_2y - iqz} \langle 0 | \mathcal{T} j_a^\mu(x) j_b^\nu(y) P_c(z) | 0 \rangle, \quad (2.67)$$

yields the non-Abelian Ward identities in momentum space

$$q_\lambda T_{abc}^{\mu\nu\lambda} = 2mT_{abc}^{\mu\nu} \quad \text{and} \quad k_{1\mu} T_{abc}^{\mu\nu\lambda} = k_{2\nu} T_{abc}^{\mu\nu\lambda} = 0. \quad (2.68)$$

⁵The reader may have noticed that there are additional conserved currents, namely $j^\mu = \bar{\psi} \gamma^\mu \psi$ and also $j_5^\mu = \bar{\psi} \gamma^\mu \gamma^5 \psi$ in the massless case. Despite the similarities with (2.13) and (2.14), these currents do not hint at a **local** Abelian gauge symmetry, but result from the fact that the example Lagrangian in (2.61) features a **global** symmetry $\psi \rightarrow e^{i\alpha} \psi$ with $\alpha = \text{const.}$

2.4.3 Anomalous non-Abelian Ward identities

2.4.3.1 Corresponding Feynman diagrams

The amplitudes given in (2.66) and (2.67) correspond to the Feynman diagrams shown in Figure 3 and Figure 4.

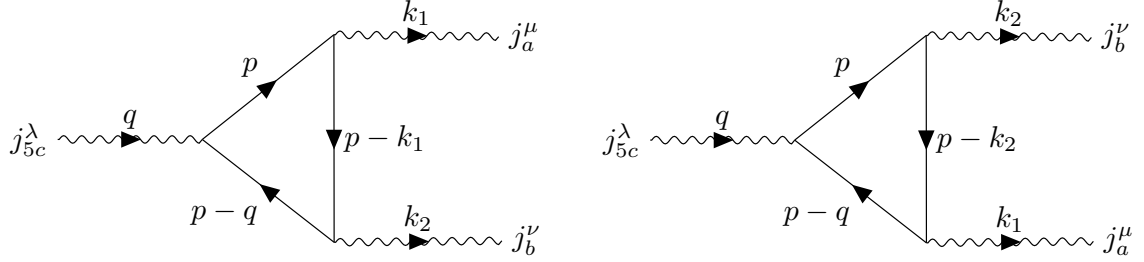


Figure 3: Contributing Feynman diagrams for $T_{abc}^{\mu\nu\lambda}$.

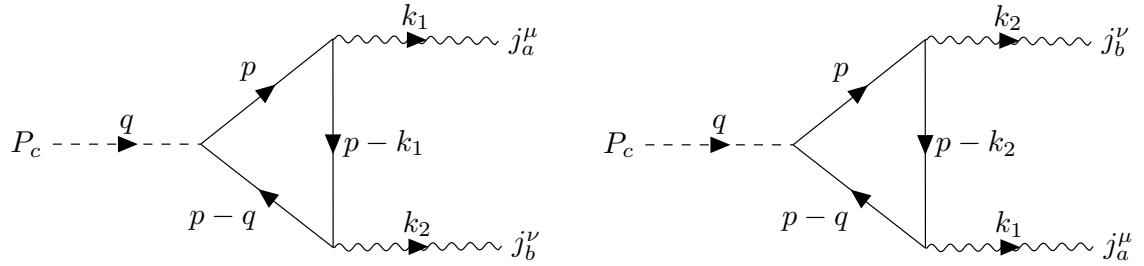


Figure 4: Contributing Feynman diagrams for $T_{abc}^{\mu\nu}$.

By the use of Feynman rules, one may recalculate the amplitudes as

$$T_{abc}^{\mu\nu\lambda} = -i \int \frac{d^4p}{(2\pi)^4} \text{Tr} \left(\frac{i}{\not{p} - m} \gamma^\lambda \gamma^5 T^c \frac{i}{\not{p} - \not{q} - m} \gamma^\nu T^b \frac{i}{\not{p} - \not{k}_1 - m} \gamma^\mu T^a \right) + \begin{pmatrix} k_1 \leftrightarrow k_2 \\ \mu \leftrightarrow \nu \\ a \leftrightarrow b \end{pmatrix} \quad (2.69)$$

$$T_{abc}^{\mu\nu} = -i \int \frac{d^4p}{(2\pi)^4} \text{Tr} \left(\frac{i}{\not{p} - m} \gamma^5 T^c \frac{i}{\not{p} - \not{q} - m} \gamma^\nu T^b \frac{i}{\not{p} - \not{k}_1 - m} \gamma^\mu T^a \right) + \begin{pmatrix} k_1 \leftrightarrow k_2 \\ \mu \leftrightarrow \nu \\ a \leftrightarrow b \end{pmatrix}. \quad (2.70)$$

2.4.3.2 Non-Abelian anomalous axial Ward identity

A comparison with the Abelian case amplitudes, (2.26) and (2.27), reveals that the first terms in (2.69) and (2.70) differ only by a factor of a trace of three generators. Hence, it is

not necessary to derive the anomalous corrections for the non-Abelian case from scratch, but one may adapt the general form of the corrections for the Abelian case, (2.36) and (2.47), yielding

$$q_\lambda T_{abc}^{\mu\nu\lambda}(0) = 2mT_{abc}^{\mu\nu}(0) + R_{abc}^{\mu\nu} \quad \text{and} \quad T_{abc}^{\mu\nu\lambda}(\beta) - T_{abc}^{\mu\nu\lambda}(0) = \Delta_{abc}^{\mu\nu\lambda}(\beta), \quad (2.71)$$

with the unshifted correction

$$R_{abc}^{\mu\nu} = \text{Tr} (T^b T^a T^c) \frac{1}{8\pi^2} \varepsilon^{\rho\mu\sigma\nu} k_{1\rho} k_{2\sigma} + \begin{pmatrix} k_1 \leftrightarrow k_2 \\ \mu \leftrightarrow \nu \\ a \leftrightarrow b \end{pmatrix} \quad (2.72)$$

$$= -\text{Tr} (\{T^a, T^b\} T^c) \frac{1}{8\pi^2} \varepsilon^{\mu\nu\rho\sigma} k_{1\rho} k_{2\sigma} \quad (2.73)$$

and the amplitude difference imposed by the loop momentum shifts, defined in (2.38),

$$\Delta_{abc}^{\mu\nu\lambda}(\beta) = \text{Tr} (T^a T^b T^c) \frac{1}{8\pi^2} [\alpha k_1 + (\alpha - \beta) k_2]_\sigma \varepsilon^{\mu\nu\lambda\sigma} + \begin{pmatrix} k_1 \leftrightarrow k_2 \\ \mu \leftrightarrow \nu \\ a \leftrightarrow b \end{pmatrix} \quad (2.74)$$

$$= -\text{Tr} (T^a T^b T^c) \frac{\beta}{8\pi^2} \varepsilon^{\mu\nu\lambda\sigma} (k_1 - k_2)_\sigma + \text{commutator terms} \quad (2.75)$$

$$= -\frac{1}{2} \text{Tr} (\{T^a, T^b\} T^c) \frac{\beta}{8\pi^2} \varepsilon^{\mu\nu\lambda\sigma} (k_1 - k_2)_\sigma + \text{commutator terms}. \quad (2.76)$$

In analogy to (2.49), one finds the anomalous axial Ward identity for the non-Abelian case:

$$q_\lambda T_{abc}^{\mu\nu\lambda}(\beta) = 2mT_{abc}^{\mu\nu} - \frac{1}{2} \text{Tr} (\{T^a, T^b\} T^c) \frac{1 - \beta}{4\pi^2} \varepsilon^{\mu\nu\rho\sigma} k_{1\rho} k_{2\sigma} + \text{commutator terms} \quad (2.77)$$

2.4.3.3 Non-Abelian ABJ anomaly

Following the argumentation in section 2.3.3.3, it is convenient to shift the anomaly to the axial Ward identity only (which is precisely why the vector identities were skipped in the above derivation). Choosing $\beta = -1$ in (2.77) yields the final result:

$$q_\lambda T_{abc}^{\mu\nu\lambda} = 2mT_{abc}^{\mu\nu} + \mathcal{A}_{abc}^{\mu\nu} + \text{commutator terms} \quad (2.78)$$

It can be shown that the commutator term are not relevant [18]. Thus, one finds the non-Abelian ABJ anomaly in momentum space (see also the Abelian result (2.60))

$$\mathcal{A}_{abc}^{\mu\nu} = -\frac{\tau_{abc}}{2\pi^2} \varepsilon^{\mu\nu\rho\sigma} k_{1\rho} k_{2\sigma}, \quad \text{where} \quad \tau_{abc} := \frac{1}{2} \text{Tr} (\{T^a, T^b\} T^c). \quad (2.79)$$

This trace factor τ_{abc} will turn out to be the relevant quantity for our study of anomalies in the remainder of this thesis.⁶

⁶The trace factor τ_{abc} is zero in so-called vector-like models, where left-handed and right-handed fermions couple symmetrically, so their contributions cancel (see for instance the QCD anomaly in (2.92)). Furthermore, there are "safe groups", for which the trace factors are automatically zero. Examples of safe groups in four dimensions are $SU(2)$, $SO(2n+1)$, $SO(4n)$ with integer $n \geq 2$, as well as the exceptional groups $E(6)$ and $E(8)$ [11].

2.5 Importance of Anomalies

The significance of anomalies depends on the nature of the symmetry that they are violating. There are two cases to consider.

Global anomalies: Anomalies that violate a global symmetry are useful in the sense that they give rise to physical observables. The most prominent example is the decay of a pion into two photons (see Figure 5):⁷

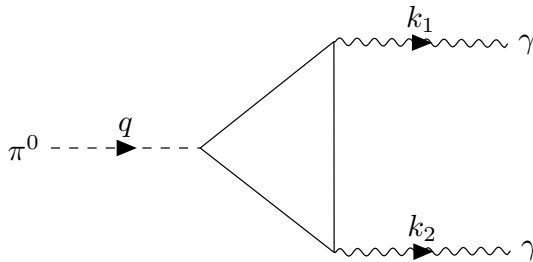


Figure 5: Decay $\pi^0(q) \rightarrow \gamma(k_1)\gamma(k_2)$ with $q = k_1 + k_2$.

Since it clearly corresponds to the triangle graphs in Figure 4, this decay is determined by the ABJ anomaly (2.79).⁸

Gauge anomalies: In contrast to global anomalies, anomalies arising in the context of gauge symmetries are quite harmful to the gauge theory. It can be shown that in the presence of gauge anomalies renormalisability is lost [21]. In addition, the S-matrix may no longer be unitary [22]. Thus, in order to have a consistent gauge theory, there must not be any gauge anomalies.

2.6 Anomalies in the Standard Model of particle physics

As highlighted by the discussion in the last chapter, gauge anomalies spoil the consistency of a quantised perturbative gauge theory like the SM. However, we will see that the SM particles contribute to the relevant triangle graphs in such a way that all anomalies vanish. First, the SM gauge group and the relevant part of the SM Lagrangian are introduced. Afterwards, the anomaly cancellation will be discussed in detail.

2.6.1 Particle content and Electroweak Lagrangian of the Standard Model

The SM shows a symmetry under the semisimple gauge group

$$SU(3)_c \times SU(2)_L \times U(1)_Y \tag{2.80}$$

⁷The decay via a triangle diagram was first discussed by Steinberger in 1949 [19].

⁸It should be mentioned that the ABJ anomaly determines this decay only up to leading order. More details may be found at [20].

composed of the local gauge groups associated with QCD ($SU(3)_c$), electroweak interactions ($SU(2)_L$) and QED ($U(1)_Y$), respectively [15]. The SM particles, formed by quarks, leptons and the Higgs particle, are arranged in multiplets or singlets under these simple groups.

Table 1 lists the SM particles and their representation under the gauge group (2.80). We use the following notation: q_L denotes the left-handed quark doublet, l_L the left-handed lepton doublet, u_R and d_R are the right-handed quark singlets, corresponding to weak isospin "up" and "down" respectively, and e_R labels the right-handed charged lepton singlet. For each particle, the upper index $i = 1, 2, 3$ labels the generation. Last but not least, the scalar Higgs boson is denoted by Φ .

	$SU(3)_c$	$SU(2)_L$	$U(1)_Y$
$q_L^i = \begin{pmatrix} u_L^i \\ d_L^i \end{pmatrix}$	3	2	$+\frac{1}{6}$
$l_L^i = \begin{pmatrix} \nu_L^i \\ e_L^i \end{pmatrix}$	1	2	$-\frac{1}{2}$
u_R^i	3	1	$+\frac{2}{3}$
d_R^i	3	1	$-\frac{1}{3}$
e_R^i	1	1	-1
Φ	1	2	$+\frac{1}{2}$

Table 1: SM particle content and representations under the gauge groups.

The electroweak Lagrangian is given as [15]:

$$\mathcal{L}_{ew} = \mathcal{L}_F + \mathcal{L}_H + \mathcal{L}_G + \mathcal{L}_Y - V(\phi). \quad (2.81)$$

\mathcal{L}_F contains the gauge-covariant derivatives of the fermion fields

$$\mathcal{L}_F = -i (\bar{q}_L \not{D} q_L + \bar{l}_L \not{D} l_L + \bar{u}_R \not{D} u_R + \bar{d}_R \not{D} d_R + \bar{e}_R \not{D} e_R), \quad (2.82)$$

with the covariant derivative given in the following way:⁹

$$D_\mu = \partial_\mu - ig_1 B_\mu T_{U(1)_Y} - ig_2 W_\mu^j T_{SU(2)_L}^j - ig_3 G_\mu^a T_{SU(3)_c}^a \quad (2.83)$$

The gauge couplings for $U(1)_Y$, $SU(2)_L$ and $SU(3)_c$ are labelled as g_1 , g_2 and g_3 , respectively. Using the generators from section 2.1 and the particle content in Table 1, the covariant

⁹This is a shorthand notation. In fact, the covariant derivative is different for each field. The second or third term are only present, if the the field acted on has a non-zero hypercharge under $SU(1)_Y$ or a non-singlet representation under $SU(2)_L$, respectively.

derivative can be written explicitly as

$$\begin{aligned}
D_\mu q_L &\equiv \left(\partial_\mu - i\frac{g_1}{6}B_\mu - i\frac{g_2}{2}\sigma^j W_\mu^j - i\frac{g_3}{2}\lambda^a G_\mu^a \right) q_L \\
D_\mu l_L &\equiv \left(\partial_\mu + i\frac{g_1}{2}B_\mu - i\frac{g_2}{2}\sigma^j W_\mu^j \right) l_L \\
D_\mu u_R &\equiv \left(\partial_\mu - i\frac{2}{3}g_1 B_\mu - i\frac{g_3}{2}\lambda^a G_\mu^a \right) u_R \\
D_\mu d_R &\equiv \left(\partial_\mu + i\frac{g_1}{3}B_\mu - i\frac{g_3}{2}\lambda^a G_\mu^a \right) d_R \\
D_\mu e_R &\equiv (\partial_\mu + ig_1 B_\mu) e_R,
\end{aligned} \tag{2.84}$$

with the Pauli matrices σ^j and Gell-Mann matrices λ^a as defined in appendix A.1.

The covariant derivatives of the Higgs field are contained in \mathcal{L}_H as

$$\mathcal{L}_H = (D_\mu \Phi)^\dagger (D^\mu \Phi) \quad \text{with} \quad D_\mu \Phi \equiv \left(\partial_\mu - i\frac{g_1}{2}B_\mu - i\frac{g_2}{2}\sigma^j W_\mu^j \right) \Phi, \tag{2.85}$$

where $\Phi = \begin{pmatrix} \phi^+ \\ \phi^0 \end{pmatrix}$ denotes the Higgs doublet.

The gauge contribution part is labelled as \mathcal{L}_G and has the form

$$\mathcal{L}_G = -\frac{1}{4}G_{\mu\nu}^a G^{a\mu\nu} - \frac{1}{4}F_{\mu\nu}^j F^{j\mu\nu} - \frac{1}{4}B_{\mu\nu} B^{\mu\nu}, \tag{2.86}$$

where

$$\begin{aligned}
G_{\mu\nu}^a &\equiv \partial_\mu G_\nu^a - \partial_\nu G_\mu^a + g_3 f^{abc} G_\mu^b G_\nu^c \\
F_{\mu\nu}^j &\equiv \partial_\mu W_\nu^j - \partial_\nu W_\mu^j + g_2 f^{jkl} W_\mu^k W_\nu^l \\
B_{\mu\nu} &\equiv \partial_\mu B_\nu - \partial_\nu B_\mu,
\end{aligned} \tag{2.87}$$

with the structure constants as given in (A.2) and (A.6).

Finally, the Yukawa couplings of the Higgs field and the fermions are contained in \mathcal{L}_Y :

$$\mathcal{L}_Y = -\bar{q}_L \Gamma \Phi d_R - \bar{q}_L \Delta \tilde{\Phi} u_R + \bar{l}_L \Pi \Phi e_R + \text{H.c.} \quad \text{with} \quad \tilde{\Phi} := i\sigma^2 \Phi^* \tag{2.88}$$

2.6.2 Anomaly cancellation in the Standard Model

In order to check for gauge anomalies, we will study the triangle graphs like in section 2.4.3 and calculate the trace factors τ_{abc} as defined in (2.79). There are three types of generators for the three parts of the gauge group:

$$T_3^a := T_{\text{SU}(3)}^a \otimes \mathbb{1}_{\text{SU}(2)} \otimes \mathbb{1}_{\text{U}(1)} \tag{2.89}$$

$$T_2^a := \mathbb{1}_{\text{SU}(3)} \otimes T_{\text{SU}(2)}^a \otimes \mathbb{1}_{\text{U}(1)} \tag{2.90}$$

$$T_1^a \equiv T_1 := \mathbb{1}_{\text{SU}(3)} \otimes \mathbb{1}_{\text{SU}(2)} \otimes T_{\text{U}(1)} \tag{2.91}$$

The anomaly triangle graphs may now contain one of the three types of these generators at each vertex. However, the order at which one puts the generators at the vertices is irrelevant, so, a priori, there are ten potential triangle anomalies.

In the following, we will label the triangle graphs by the groups participating. For instance, the anomaly denoted by $[\text{SU}(3)]^2 \times \text{U}(1)$ corresponds to the generator assignment in Figure 6.

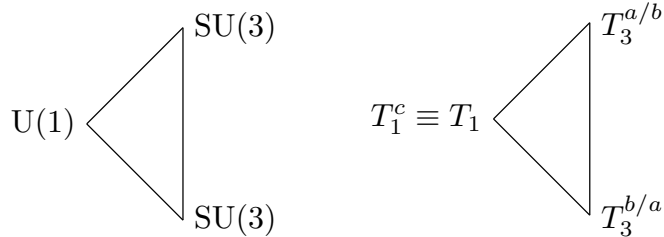


Figure 6: Triangle graph and generator assignment for the $[\text{SU}(3)]^2 \times \text{U}(1)$ anomaly.

Five of the anomalies vanish trivially, because the generators of $\text{SU}(3)$ and $\text{SU}(2)$ are traceless (see appendix (A.6)). The remaining ones will be discussed here.

At each graph, only particles with non-singlet representations under *all* the participating groups will enter.¹⁰ The final value of the anomaly is acquired by summing over all the contributing particles and their degrees of freedom.

Due to different chirality, right-handed particles will enter with an overall minus sign compared to the left-handed particles ([21] for more details). Using the SM particle content, as given in Table 1, one finds¹¹

$$\begin{aligned}
 [\text{SU}(3)]^3 &\propto \sum_{\text{d.o.f.}} \text{Tr} (\{T_3^a, T_3^b\} T_3^c) = \\
 &= \text{Tr} (\{T_3^a, T_3^b\} T_3^c) \sum_{i=1}^3 \left(\underbrace{3 \cdot 2}_{q_L^i} - \left(\underbrace{3 \cdot 1}_{u_R^i} + \underbrace{3 \cdot 1}_{d_R^i} \right) \right) \equiv 0,
 \end{aligned} \tag{2.92}$$

$$\begin{aligned}
 [\text{SU}(3)]^2 \times \text{U}(1) &\propto \sum_{\text{d.o.f.}} \text{Tr} (\{T_3^a, T_3^b\} T_1^c) = \\
 &= \text{Tr} \{T_3^a, T_3^b\} \sum_{i=1}^3 \left(\underbrace{\frac{1}{6} \cdot 2}_{q_L^i} - \left(\underbrace{\frac{2}{3} \cdot 1}_{u_R^i} + \underbrace{\left(-\frac{1}{3}\right) \cdot 1}_{d_R^i} \right) \right) \equiv 0,
 \end{aligned} \tag{2.93}$$

¹⁰In the case of $\text{U}(1)$, this means non-zero hypercharge.

¹¹The scalar Higgs field does not enter the anomaly equations. This is due to the fact that only fermionic loops lead to linear divergent integrals as (2.26) or (2.69). Replacing the fermionic propagators $\frac{i}{\not{p}-\not{m}}$ by scalar ones $\frac{i}{p^2-m^2}$, as it would be for the Higgs field, yields convergent integrals, hence no contribution to the anomaly.

as well as

$$\begin{aligned}
[\text{SU}(2)]^2 \times \text{U}(1) &\propto \sum_{\text{d.o.f.}} \text{Tr} (\{T_2^a, T_2^b\} T_1^c) = \\
&= \text{Tr} \{T_2^a, T_2^b\} \sum_{i=1}^3 \left(\underbrace{\left(\frac{1}{6}\right)^3 \cdot 3}_{q_L^i} + \underbrace{\left(-\frac{1}{2}\right)^3 \cdot 1}_{l_L^i} \right) \equiv 0
\end{aligned} \tag{2.94}$$

$$\begin{aligned}
\text{and } [\text{U}(1)]^3 &\propto \sum_{i=1}^3 \left[\underbrace{\left(\frac{1}{6}\right)^3 \cdot 3 \cdot 2}_{q_L^i} + \underbrace{\left(-\frac{1}{2}\right)^3 \cdot 1 \cdot 2}_{l_L^i} \right. \\
&\quad \left. - \left(\underbrace{\left(\frac{2}{3}\right)^3 \cdot 3 \cdot 1}_{u_R^i} + \underbrace{\left(-\frac{1}{3}\right)^3 \cdot 3 \cdot 1}_{d_R^i} + \underbrace{(-1)^3 \cdot 1 \cdot 1}_{e_R^i} \right) \right] \equiv 0.
\end{aligned} \tag{2.95}$$

As mentioned before, SU(2) is a safe group, which means that the $[\text{SU}(2)]^3$ anomaly is zero, independent from the particle content. This can be seen directly, since

$$\begin{aligned}
[\text{SU}(2)]^3 &\propto \sum_{\text{d.o.f.}} \text{Tr} (\{T_2^a, T_2^b\} T_2^c) = \\
&= \sum_{\text{d.o.f.}} \text{Tr} (\mathbb{1}_{\text{SU}(3)} \otimes \{T_{\text{SU}(2)}^a, T_{\text{SU}(2)}^b\} T_{\text{SU}(2)}^c \otimes \mathbb{1}_{\text{U}(1)}) = \\
&= \sum_{\text{d.o.f.}} \text{Tr} (\mathbb{1}_{\text{SU}(3)}) \text{Tr} (\{T_{\text{SU}(2)}^a, T_{\text{SU}(2)}^b\} T_{\text{SU}(2)}^c) \text{Tr} (\mathbb{1}_{\text{U}(1)}) = \\
&= \sum_{\text{d.o.f.}} \text{Tr} (\mathbb{1}_{\text{SU}(3)}) \text{Tr} \left(\frac{1}{8} \underbrace{\{\sigma^a, \sigma^b\}}_{=2\delta^{ab}\mathbb{1}_2} \sigma^c \right) \text{Tr} (\mathbb{1}_{\text{U}(1)}) \propto \text{Tr} (\sigma^c) \equiv 0,
\end{aligned} \tag{2.96}$$

where the definition of the generators for SU(2) (2.3) and the vanishing trace of the Pauli matrices have been used (see also appendix A.1).

In order to complete the discussion, one should also add gravitational anomalies, where all particles with non-zero mass enter. Gravity acts as a SO(4) group, so the corresponding generators are traceless (see appendix A.6). This implies that the only two non-trivial anomalies are $[\text{gravity}]^2 \times \text{U}(1)$ and $[\text{gravity}]^3$. However, it can be shown that purely gravitational anomalies occur only in $4n + 2$ dimensions, with $n \in \mathbb{N}$ (for a detailed

discussion see [14]). Thus, in four dimensions, there is only one gravitational anomaly:

$$\begin{aligned}
 [\text{gravity}]^2 \times \text{U}(1) \propto \sum_{i=1}^3 & \left[\underbrace{\frac{1}{6} \cdot 3 \cdot 2}_{q_L^i} + \underbrace{\left(-\frac{1}{2}\right) \cdot 1 \cdot 2}_{l_L^i} \right. \\
 & \left. - \left(\underbrace{\frac{2}{3} \cdot 3 \cdot 1}_{u_R^i} + \underbrace{\left(-\frac{1}{3}\right) \cdot 3 \cdot 1}_{d_R^i} + \underbrace{(-1) \cdot 1 \cdot 1}_{e_R^i} \right) \right] \equiv 0
 \end{aligned} \tag{2.97}$$

As a final remark of this section, please note that not only do all the anomalies cancel, but they cancel without performing the summation over the family index i . This means that the anomalies cancel for each generation of particles individually, which is an important feature of the SM.¹²

¹²In fact, incomplete gauge anomaly cancellation was one of the hints that led theoretical physicists to the prediction of the top quark, before it was discovered experimentally in the mid 90's [23].

3 Abelian symmetries in the 2HDM

3.1 The two-Higgs-doublet model in more detail

For the discussion of the 2HDM, we will restrict our attention to the Yukawa sector. Starting from the SM Yukawa Lagrangian (2.88), one finds its general form in the 2HDM

$$\mathcal{L}_{\text{Y2HDM}} = -\bar{q}_L(\Gamma_1\Phi_1 + \Gamma_2\Phi_2)d_R - \bar{q}_L(\Delta_1\tilde{\Phi}_1 + \Delta_2\tilde{\Phi}_2)u_R - \bar{l}_L(\Pi_1\Phi_1 + \Pi_2\Phi_2)e_R + \text{H.c.}, \quad (3.1)$$

with the two Higgs doublets

$$\Phi_1 = \begin{pmatrix} \phi_1^+ \\ \frac{1}{\sqrt{2}}(v_1 + (\rho_1 + i\eta_1)) \end{pmatrix} \quad \text{and} \quad \Phi_2 = \begin{pmatrix} \phi_2^+ \\ \frac{1}{\sqrt{2}}(v_2 + (\rho_2 + i\eta_2)) \end{pmatrix}, \quad (3.2)$$

where $v_{1/2}$ denote the complex vacuum expectation values (VEVs hereafter) of $\Phi_{1/2}$, respectively. They are related to the SM VEV v via

$$|v_1|^2 + |v_2|^2 = |v|^2 = (246 \text{ GeV})^2. \quad (3.3)$$

The corresponding Yukawa matrices are labelled $\Gamma_{1/2}$, $\Delta_{1/2}$, $\Pi_{1/2}$. Accordingly, after electroweak spontaneous symmetry breaking, the mass matrices for down and up type quarks are given as

$$M_d = \frac{1}{\sqrt{2}}(v_1\Gamma_1 + v_2\Gamma_2) \quad \text{and} \quad M_u = \frac{1}{\sqrt{2}}(v_1^*\Delta_1 + v_2^*\Delta_2). \quad (3.4)$$

Both mass matrices can be bi-diagonalised as

$$V_{dL}^\dagger M_d V_{dR} = D_d = \begin{pmatrix} m_d & & \\ & m_s & \\ & & m_b \end{pmatrix} \quad \text{and} \quad V_{uL}^\dagger M_u V_{uR} = D_u = \begin{pmatrix} m_u & & \\ & m_c & \\ & & m_t \end{pmatrix}, \quad (3.5)$$

with the quark masses for down m_d , strange m_s , bottom m_b , as well as for up m_u , charm m_c and top m_t . The unitary matrices V_{dL} , V_{dR} and V_{uL} , V_{uR} correspond to the transformation from flavour to the mass basis for the left- and right-handed quarks in down and up sector, respectively:¹³

$$d_L \rightarrow V_{dL}d_L \quad d_R \rightarrow V_{dR}d_R \quad u_L \rightarrow V_{uL}u_L \quad u_R \rightarrow V_{uR}u_R \quad (3.6)$$

At this point, it is convenient to define the two Hermitian matrices

$$H_d := M_d M_d^\dagger = \frac{1}{2} \left(|v_1|^2 \Gamma_1 \Gamma_1^\dagger + |v_2|^2 \Gamma_2 \Gamma_2^\dagger + v_1 v_2^* \Gamma_1 \Gamma_2^\dagger + v_1^* v_2 \Gamma_2 \Gamma_1^\dagger \right) \quad (3.7)$$

$$H_u := M_u M_u^\dagger = \frac{1}{2} \left(|v_1|^2 \Delta_1 \Delta_1^\dagger + |v_2|^2 \Delta_2 \Delta_2^\dagger + v_1^* v_2 \Delta_1 \Delta_2^\dagger + v_1 v_2^* \Delta_2 \Delta_1^\dagger \right), \quad (3.8)$$

¹³These transformations have to be unitary in order to keep the kinetic terms of the Lagrangian canonical.

which are diagonalised by only one matrix each:

$$V_{\text{dL}}^\dagger H_{\text{d}} V_{\text{dL}} = D_{\text{d}}^2 \quad \text{and} \quad V_{\text{uL}}^\dagger H_{\text{u}} V_{\text{uL}} = D_{\text{u}}^2 \quad (3.9)$$

In order to be consistent, the transformation from flavour to mass basis also has to be applied to the derivative terms of the fermions in the Lagrangian (2.82).¹⁴ As a representative, consider the $-i\bar{q}_{\text{L}} \not{D} q_{\text{L}}$ term, which contains

$$-\frac{g_2}{\sqrt{2}} \bar{u}_{\text{L}} \gamma^\mu W_\mu^+ d_{\text{L}} \quad \text{with} \quad W_\mu^+ := \frac{W_\mu^1 - iW_\mu^2}{\sqrt{2}} \quad (3.10)$$

(see [24] for more details). Given the unitary transformations to the mass basis (3.6), one finds

$$-\frac{g_2}{\sqrt{2}} \bar{u}_{\text{L}} \gamma^\mu W_\mu^+ d_{\text{L}} \rightarrow -\frac{g_2}{\sqrt{2}} \bar{u}_{\text{L}} \gamma^\mu W_\mu^+ V_{\text{CKM}} d_{\text{L}}, \quad (3.11)$$

where V_{CKM} denotes the famous Cabibbo–Kobayashi–Maskawa (CKM) matrix, given as

$$V_{\text{CKM}} = V_{\text{uL}}^\dagger V_{\text{dL}}. \quad (3.12)$$

3.1.1 Abelian global symmetries in the 2HDM quark sector

The most general Abelian global symmetry in the 2HDM quark sector is a flavour-dependent U(1) symmetry, given by the transformation (no Einstein summation convention)

$$\begin{aligned} q_{\text{L}}^k &\rightarrow e^{i\alpha q_k} q_{\text{L}}^k & d_{\text{R}}^k &\rightarrow e^{i\alpha d_k} d_{\text{R}}^k & \Phi_1 &\rightarrow e^{i\alpha\varphi_1} \Phi_1 & \Phi_2 &\rightarrow e^{i\alpha\varphi_2} \Phi_2, \\ u_{\text{R}}^k &\rightarrow e^{i\alpha u_k} u_{\text{R}}^k & & & & & & \end{aligned} \quad (3.13)$$

parametrised by the global parameter α . The charges are denoted as φ_1, φ_2 for the Higgs doublets and q_k, d_k, u_k label the family-dependent quark charges with $k = 1, 2, 3$. Consider, for example, the first term of the Lagrangian (3.1). It transforms as

$$-\bar{q}_{\text{L}} \Gamma_1 \Phi_1 d_{\text{R}} \equiv -\Gamma_1^{jk} \bar{q}_{\text{L}}^j \Phi_1 d_{\text{R}}^k \rightarrow -\Gamma_1^{jk} e^{i\alpha(-q_j + d_k + \varphi_1)} \bar{q}_{\text{L}}^j \Phi_1 d_{\text{R}}^k. \quad (3.14)$$

Any term that is present in the Lagrangian has to be invariant under the symmetry transformations. This implies that the complex entries of the first down sector Yukawa matrix can only be non-zero, if the phases imposed on the corresponding term cancel:¹⁵

$$\Gamma_1^{jk} \neq 0 \quad \text{only if} \quad e^{i\alpha(-q_j + d_k + \varphi_1)} = 1, \forall \alpha \quad \Leftrightarrow \quad -q_j + d_k + \varphi_1 = 0 \quad (3.15)$$

The same argument goes for the other terms and Yukawa matrices in (3.1), so one may conclude:

Imposing a symmetry of type (3.13) fixes the non-zero Yukawa entries.

¹⁴This part of the 2HDM Lagrangian is identical to the SM.

¹⁵We have chosen to work with continuous symmetries, only. For a study of also discrete symmetries (i.e. discrete values of α), the condition reads $\alpha(-q_j + d_k + \varphi_1) = m \cdot 2\pi$ with integer m .

Each pattern of non-zero entries in the Yukawa matrices imposed by the symmetry (textures hereafter) reduces the amount of free parameters for the corresponding model. This is crucial for the in-depth study of a theory, because less parameters improve the ability of a model to provide predictions of physical observables. These predictions may then be tested, thus allowing for a verification of the model.

3.1.2 Finding physically relevant textures for the quark sector

For the quark sector, there are a priori 3^{18} possible Yukawa textures.¹⁶ However, in 2011 Ferreira and Silva [9] demonstrated that the amount of physically relevant textures is significantly smaller, as will be presented in the following.

As a starting point, consider a matrix that contains the nine quark phase differences under transformation (3.13) for the down sector of the Yukawa Lagrangian (3.1)

$$\Theta_{\text{down}} := \begin{pmatrix} -q_1 + d_1 & -q_1 + d_2 & -q_1 + d_3 \\ -q_2 + d_1 & -q_2 + d_2 & -q_2 + d_3 \\ -q_3 + d_1 & -q_3 + d_2 & -q_3 + d_3 \end{pmatrix}. \quad (3.16)$$

This matrix corresponds to the phase combination presented in (3.14) and (3.15), but without the Higgs phase. We will refer to it as the phase matrix of the down sector. Analogously, one may define the phase matrix for the up sector in the form of

$$\Theta_{\text{up}} := \begin{pmatrix} -q_1 + u_1 & -q_1 + u_2 & -q_1 + u_3 \\ -q_2 + u_1 & -q_2 + u_2 & -q_2 + u_3 \\ -q_3 + u_1 & -q_3 + u_2 & -q_3 + u_3 \end{pmatrix}. \quad (3.17)$$

With these definitions in mind, one can study different symmetries by imposing constraints on the charges. The idea is to create equal entries in the phase matrices, because the patterns formed by these equal entries will contain the non-zero textures of the Yukawa matrices. This may be more easily understood when looking at a simple example.

Consider, for instance, the case

$$q_1 = q_2 = q_3 \quad \text{and} \quad d_1 = d_2 \neq d_3. \quad (3.18)$$

The corresponding phase matrix for the down sector is given as

$$\Theta_{\text{down}}|_{q_1=q_2=q_3, d_1=d_2} = \begin{pmatrix} -q_1 + d_1 & -q_1 + d_1 & -q_1 + d_3 \\ -q_1 + d_1 & -q_1 + d_1 & -q_1 + d_3 \\ -q_1 + d_1 & -q_1 + d_1 & -q_1 + d_3 \end{pmatrix}. \quad (3.19)$$

¹⁶For the down sector, each of the nine entries has three possibilities. It is either zero, non-zero in Γ_1 or non-zero in Γ_2 . A similar counting can be applied to the up sector. Because both sectors are independent, there is a total of $3^9 \cdot 3^9$ possibilities.

It is evident that, in this case, there are only two different quark phases for the down sector: $-q_1 + d_1$ and $-q_1 + d_3$. These two phases may now be set equal to minus the two Higgs charges, for instance

$$-q_1 + d_1 = -\varphi_1 \quad \text{and} \quad -q_1 + d_3 = -\varphi_2, \quad (3.20)$$

which implies that in the overall phases for the corresponding entries cancel, as discussed for the example case (3.15). Consequently, the patterns of the equal entries match the non-zero textures of the down Yukawa matrices, namely

$$\Gamma_1 = \begin{pmatrix} \mathbf{x} & \mathbf{x} & 0 \\ \mathbf{x} & \mathbf{x} & 0 \\ \mathbf{x} & \mathbf{x} & 0 \end{pmatrix} \quad \text{and} \quad \Gamma_2 = \begin{pmatrix} 0 & 0 & \mathbf{x} \\ 0 & 0 & \mathbf{x} \\ 0 & 0 & \mathbf{x} \end{pmatrix}, \quad (3.21)$$

where \mathbf{x} labels a general complex entry of any value. Please note that these entries may be all different, but not zero. Of course, one may have chosen the opposite Higgs charges for phase cancellation in (3.20), i.e. $\varphi_1 \leftrightarrow \varphi_2$. Still, the phase matrix would contain the Yukawa textures presented in (3.21), only with the switch $\Gamma_1 \leftrightarrow \Gamma_2$.

In a more general case (more different charges), the symmetry may impose more than two textures on the phase matrix, which allows for more than two identifications of the Higgs charges. However, many "equal entry" patterns give unphysical results when used as non-zero textures for the Yukawa matrices, which is what has been studied by [9] and will be discussed briefly in the remainder of this section.

In order to ensure that the textures are physically valid, two conditions were applied. First, any combination of two textures (for the two Higgs doublets respectively) that led to at least one massless quark was ruled out.¹⁷ The mathematical formulation of this constraint is that both mass matrices (3.4) have to have a non-vanishing determinant, which reads¹⁸

$$\det M_d \stackrel{!}{\neq} 0 \quad \text{and} \quad \det M_u \stackrel{!}{\neq} 0. \quad (3.22)$$

As a second condition, the textures had to allow sufficient quark mixing. For this purpose, it was checked that there are no block-diagonal structures in the CKM matrix (3.12).

Applying these two conditions allowed [9] to reduce the number of textures to 246.

3.2 Promoting the global symmetries to a gauge symmetries

Unfortunately, the reduction of free parameters via the additional U(1) symmetry (3.13) and the corresponding texture choices, as discussed in section 3.1.1, comes with a price:

¹⁷Due to the strong hierarchy of quark masses, one might want to work in the approximation of massless down and up quarks, when compared to bottom and top quarks, respectively. However, this was not considered in the original analysis of [9] and is likewise omitted from the discussion of this thesis.

¹⁸The notation [!] indicates that the relation does not apply in general but is imposed as a condition. In other words, we *demand* the determinant to be non-zero.

Spontaneous symmetry breaking, as presented in the beginning of section 3.1, is an essential part of the 2HDM. In analogy to the SM, it is this very mechanism that provides masses for the gauge bosons [3]. However, any spontaneously broken *global* symmetry gives rise to a massless Goldstone boson (see appendix A.7), which has not been observed experimentally.

There are two ways to deal with this problem. One option is to add a *soft breaking term*, that violates the symmetry. The underlying idea is that the theory is still renormalisable if the symmetry breaking term has a dimension less than 4 [25].

A more elegant way is to promote the global symmetry to a gauge symmetry with a massive gauge boson. The degree of freedom provided by the massless Goldstone boson is then absorbed into the longitudinal polarisation of the gauge boson [10]. However, this also promotes initially global anomalies to gauge anomalies. As highlighted in section 2.5, gauge anomalies spoil the consistency of a theory and one has to make sure that they cancel.

In this thesis, we will study the 246 textures, as found by [9], in the context of gauge anomalies and see if they allow for anomaly cancellation.

3.2.1 Extended gauge group and anomaly equations

The gauge group is an extension of SM gauge group by the added $U(1)'$ group:

$$SU(3)_c \times SU(2)_L \times U(1)_Y \times U(1)' \quad (3.23)$$

Consequently, the covariant derivative becomes (see also SM case (2.83))

$$D_\mu = \partial_\mu - ig_1 B_\mu T_{U(1)_Y} - ig_2 W_\mu^j T_{SU(2)_L}^j - ig_3 G_\mu^a T_{SU(3)_c}^a - ig_1' B_\mu' T_{U(1)'}, \quad (3.24)$$

where g_1' denotes the gauge coupling for the new $U(1)'$ gauge group.

The full particle content and representations under the extended gauge group (3.23) are listed in Table 2.

	$SU(3)_c$	$SU(2)_L$	$U(1)_Y$	$U(1)'$
$q_L^i = \begin{pmatrix} u_L^i \\ d_L^i \end{pmatrix}$	3	2	$+\frac{1}{6}$	q_i
$l_L^i = \begin{pmatrix} \nu_L^i \\ e_L^i \end{pmatrix}$	1	2	$-\frac{1}{2}$	l_i
u_R^i	3	1	$+\frac{2}{3}$	u_i
d_R^i	3	1	$-\frac{1}{3}$	d_i
e_R^i	1	1	-1	e_i
$\Phi_{1,2}$	1	2	$+\frac{1}{2}$	$\varphi_{1,2}$

Table 2: Particle content for $SM \times U(1)'$. $U(1)'$ charges are family-dependent.

In accordance with the global symmetry transformation (3.13), the charges of the particles under this $U(1)'$ group are also family-dependent. The symmetry transformations are given by¹⁹

$$\begin{aligned} q_L^k &\rightarrow e^{i\alpha(x)q_k} q_L^k & d_R^k &\rightarrow e^{i\alpha(x)d_k} d_R^k & l_L^k &\rightarrow e^{i\alpha(x)l_k} l_L^k & e_R^k &\rightarrow e^{i\alpha(x)e_k} e_R^k, \end{aligned} \quad (3.25)$$

$$\begin{aligned} u_R^k &\rightarrow e^{i\alpha(x)u_k} u_R^k \end{aligned}$$

with the family index k and the - now space-time dependent - parameter $\alpha(x)$. Furthermore, the two Higgs doublets transform as

$$\Phi_1 \rightarrow e^{i\alpha(x)\varphi_1} \Phi_1 \quad \text{and} \quad \Phi_2 \rightarrow e^{i\alpha(x)\varphi_2} \Phi_2. \quad (3.26)$$

As demonstrated in section 2.6.2, there are no anomalies in the SM. Consequently, only anomalies with at least one participating $U(1)'$ have to be investigated. Removing the trivially cancelling anomalies yields a total of six relevant anomalies

$$\begin{aligned} [\text{SU}(3)]^2 \times U(1)' &\propto A_{331'} & [\text{SU}(2)]^2 \times U(1)' &\propto A_{221'} \\ [U(1)]^2 \times U(1)' &\propto A_{111'} & [\text{gravity}]^2 \times U(1)' &\propto A_{\text{gg}1'} \\ U(1) \times [U(1)']^2 &\propto A_{11'1'} & [U(1)']^3 &\propto A_{1'1'1'}, \end{aligned} \quad (3.27)$$

with the anomaly coefficients given as

$$\begin{aligned} A_{331'} &= \sum_{i=1}^3 (2q_i - u_i - d_i) & A_{221'} &= \sum_{i=1}^3 (3q_i + l_i) \\ A_{111'} &= \sum_{i=1}^3 (q_i + 3l_i - 8u_i - 2d_i - 6e_i) & A_{\text{gg}1'} &= \sum_{i=1}^3 (6q_i + 2l_i - 3u_i - 3d_i - e_i) \end{aligned} \quad (3.28)$$

and

$$\begin{aligned} A_{11'1'} &= \sum_{i=1}^3 (q_i^2 - l_i^2 - 2u_i^2 + d_i^2 + e_i^2) \\ A_{1'1'1'} &= \sum_{i=1}^3 (6q_i^3 + 2l_i^3 - 3u_i^3 - 3d_i^3 - e_i^3). \end{aligned} \quad (3.29)$$

Setting all anomaly coefficients to zero yields a set of up to six independent equations. This is what will be referred to as the anomaly equations.

¹⁹No Einstein summation convention.

4 Implementation of anomaly cancellation into the 2HDM and resulting models

The following section covers the preliminary considerations and details on how the anomaly cancellation was implemented numerically for the models extracted from [9]. We start with an investigation of the quark sector and end with a similar study for the combined quark and lepton sector. Many of the technical details apply for both parts, so they are discussed extensively for the "quarks only" scenario and covered more concisely in the combined "quarks and leptons" case.

4.1 Quark sector only

In this section, we will only study the quark sector of the Yukawa Lagrangian. Although the anomaly equations simplify in the absence of leptons, this does not mean that generality is lost. In fact, any of these models can trivially be extended by a lepton sector, as will be discussed in the end of section 4.1.7.

4.1.1 Lagrangian and anomaly equations for the quark sector

For our study of the quark sector, the Yukawa Lagrangian (3.1) simplifies:

$$\mathcal{L}_{\text{Y2HDM}}|_{\text{quarks}} = -\bar{q}_L(\Gamma_1\Phi_1 + \Gamma_2\Phi_2)d_R - \bar{q}_L(\Delta_1\tilde{\Phi}_1 + \Delta_2\tilde{\Phi}_2)u_R + \text{H.c.} \quad (4.1)$$

In the absence of leptons ($l_i = e_i = 0, \forall i$), the anomaly equations imposed by (3.28) and (3.29) reduce to a set of five independent equations:²⁰

$$\left. \begin{aligned} 0 \stackrel{!}{=} A_{331'} &= \sum_{i=1}^3 (2q_i - u_i - d_i) \equiv \frac{1}{3}A_{\text{gg}1'} \\ 0 \stackrel{!}{=} A_{221'} &= \sum_{i=1}^3 3q_i \\ 0 \stackrel{!}{=} A_{111'} &= \sum_{i=1}^3 (q_i - 8u_i - 2d_i) \\ 0 \stackrel{!}{=} A_{11'1'} &= \sum_{i=1}^3 (q_i^2 - 2u_i^2 + d_i^2) \\ 0 \stackrel{!}{=} A_{1'1'1'} &= \sum_{i=1}^3 (6q_i^3 - 3u_i^3 - 3d_i^3) \end{aligned} \right\} \Leftrightarrow \left\{ \begin{aligned} 0 \stackrel{!}{=} \sum_{i=1}^3 q_i \\ 0 \stackrel{!}{=} \sum_{i=1}^3 d_i \\ 0 \stackrel{!}{=} \sum_{i=1}^3 u_i \\ 0 \stackrel{!}{=} \sum_{i=1}^3 (q_i^2 - 2u_i^2 + d_i^2) \\ 0 \stackrel{!}{=} \sum_{i=1}^3 (2q_i^3 - u_i^3 - d_i^3) \end{aligned} \right. \quad (4.2)$$

²⁰Using the same notation as before, the symbol $\stackrel{!}{=}$ emphasises that the equality is imposed as a condition at this point. In other words, we *want* all anomaly coefficients to be zero (anomaly cancellation).

4.1.2 Using textures as a starting point

In order to implement all potential models, we extracted the textures from [9] that correspond to continuous symmetry transformations. Discrete symmetries were neglected. This yielded a total of four classes, given by the general form of the phase matrices:

$$\text{Class I: } \Theta = \begin{pmatrix} a & b & c \\ a - 2\theta & b - 2\theta & c - 2\theta \\ a - \theta & b - \theta & c - \theta \end{pmatrix} \Rightarrow 8 \text{ independent texture pairs} \quad (4.3)$$

$$\text{Class II: } \Theta = \begin{pmatrix} a & b & c \\ a & b & c \\ a & b & c \end{pmatrix} \Rightarrow 4 \text{ independent texture pairs} \quad (4.4)$$

$$\text{Class III: } \Theta = \begin{pmatrix} a & b & c \\ a & b & c \\ a + \theta & b + \theta & c + \theta \end{pmatrix} \Rightarrow 6 \text{ independent texture pairs} \quad (4.5)$$

$$\text{Class IV: } \Theta = \begin{pmatrix} a & b & c \\ a & b & c \\ a - \theta & b - \theta & c - \theta \end{pmatrix} \Rightarrow 6 \text{ independent texture pairs} \quad (4.6)$$

At this, a , b , c are free parameters. Class III (4.5) and IV (4.6) show up as two distinct classes, because in their derivation [9] kept only one Higgs charge as a parameter θ while the other one was fixed to be zero.

In our analysis, however, we did not fix the Higgs charges (in fact any of the charges) but started from the textures. One might say that we inverted the procedure of [9]. There, one started with the most general symmetry, imposed charges and derived the physical textures. What we did instead is, we used their final textures (which have to correspond to a symmetry, because that is what they were derived from in the first place) and checked, if they give enough freedom for the charges to solve the anomaly equations.

This implies that class III (4.5) and IV (4.6) are identical for us, because they feature the same textures, only derived from different charge assignments. Within each class, any two texture pairs may be combined to serve as the down and the up Yukawa textures. Consequently, we considered $8^2 + 4^2 + 6^2 = 116$ texture combinations as our potential models.

4.1.3 Numerical procedure to rule out models

The computations of this thesis were done in Mathematica 11.²¹

Similar to [9], we started out with the phase matrices (3.16) and (3.17) in their most general form. As our first step, the constraints imposed by the Yukawa textures were derived for each model and applied to the phase matrices. Correspondingly, this meant that some of the - initially free - charges were constrained.

²¹Wolfram Research, Inc., Mathematica, Version 11.0, Champaign, IL (2016).

Using the constrained charges, the anomaly equations (4.2) were applied to each model in two steps. First, only the linear anomaly equations were solved. In the next step, the quadratic and cubic equations were solved, thus providing up to six solutions.

After each step, the derived relations between the charges were applied to the phase matrices (3.16), (3.17) and we checked if the original textures were still present. This is necessary, because some solutions might cause other entries to take values equal to (minus) one of the Higgs charges, which would then correspond to a different model.

In order to finally distinguish between "good" and "bad" models, an additional condition was applied: Based on a group theoretical argument, the solution to the anomaly equations has to allow all charges to be rational numbers.²²

In summary, only if the anomaly equations (4.2) could be solved with rational charges *and* if, under this solution, the phase matrices still contained the initial textures, a model was classified "good". All other models were ruled out.

Example of a "good" model: Consider the textures

$$\Gamma_1 : \begin{pmatrix} \mathbf{x} & 0 & 0 \\ 0 & \mathbf{x} & 0 \\ 0 & 0 & \mathbf{x} \end{pmatrix} \quad \Gamma_2 : \begin{pmatrix} 0 & 0 & \mathbf{x} \\ 0 & 0 & 0 \\ 0 & \mathbf{x} & 0 \end{pmatrix} \quad \Delta_1 : \begin{pmatrix} \mathbf{x} & 0 & 0 \\ 0 & 0 & \mathbf{x} \\ 0 & \mathbf{x} & 0 \end{pmatrix} \quad \Delta_2 : \begin{pmatrix} 0 & 0 & 0 \\ 0 & \mathbf{x} & 0 \\ \mathbf{x} & 0 & 0 \end{pmatrix}. \quad (4.7)$$

- Imposing the textures as equal entries on the phase matrices (3.16) and (3.17) yields

$$\left. \begin{array}{l} -q_1 + d_1 = -q_2 + d_2 \\ -q_1 + d_1 = -q_3 + d_3 \\ -q_1 + d_3 = -q_3 + d_2 \end{array} \right\} \Leftrightarrow \begin{cases} q_1 = q_2 + 2d_1 - 2d_3 \\ q_3 = q_2 + d_1 - d_3 \\ d_2 = -d_1 + 2d_3 \end{cases} \quad (4.8)$$

for the down sector and

$$\left. \begin{array}{l} -q_1 + u_1 = -q_2 + u_3 \\ -q_1 + u_1 = -q_3 + u_2 \\ -q_2 + u_2 = -q_3 + u_1 \end{array} \right\} \Leftrightarrow \begin{cases} q_1 = -q_2 + 2q_3 \\ u_1 = -q_2 + q_3 + u_2 \\ u_3 = q_2 - q_3 + u_2 \end{cases} \quad (4.9)$$

for the up sector. Substituting relations (4.8) and (4.9) into the corresponding phase matrix yields

$$\Theta_{\text{down}}|_{\text{textures}} = \begin{pmatrix} -q_2 - d_1 + 2d_3 & -q_2 - 3d_1 + 4d_3 & -q_2 - 2d_3 + 3d_3 \\ -q_2 + d_1 & -q_2 - d_1 + 2d_3 & -q_2 + d_3 \\ -q_2 + d_3 & -q_2 - 2d_3 + 3d_3 & -q_2 - d_1 + 2d_3 \end{pmatrix} \quad (4.10)$$

$$\Theta_{\text{up}}|_{\text{textures}} = \begin{pmatrix} -q_3 + u_2 & q_2 - 2q_3 + u_2 & 2q_2 - 3q_3 + u_2 \\ -2q_2 + q_3 + u_2 & -q_2 + u_2 & -q_3 + u_2 \\ -q_2 + u_2 & -q_3 + u_2 & q_2 - 2q_3 + u_2 \end{pmatrix}. \quad (4.11)$$

²²This is because the $U(1)'$ group can only be compact, if none of the charges is irrational [26]. Please note that the restriction to rational charges equates to integer charges, if some suitable normalisation is chosen.

Accordingly, the patterns formed by the equal entries are:

$$\Theta_{\text{down}} : \begin{pmatrix} \mathbf{x} & 0 & 0 \\ 0 & \mathbf{x} & 0 \\ 0 & 0 & \mathbf{x} \end{pmatrix}, \begin{pmatrix} 0 & 0 & \mathbf{x} \\ 0 & 0 & 0 \\ 0 & \mathbf{x} & 0 \end{pmatrix}, \begin{pmatrix} 0 & 0 & 0 \\ 0 & 0 & \mathbf{x} \\ \mathbf{x} & 0 & 0 \end{pmatrix}, \begin{pmatrix} 0 & 0 & 0 \\ \mathbf{x} & 0 & 0 \\ 0 & 0 & 0 \end{pmatrix}, \begin{pmatrix} 0 & \mathbf{x} & 0 \\ 0 & 0 & 0 \\ 0 & 0 & 0 \end{pmatrix} \quad (4.12)$$

$$\Theta_{\text{up}} : \begin{pmatrix} \mathbf{x} & 0 & 0 \\ 0 & 0 & \mathbf{x} \\ 0 & \mathbf{x} & 0 \end{pmatrix}, \begin{pmatrix} 0 & \mathbf{x} & 0 \\ 0 & 0 & 0 \\ 0 & 0 & \mathbf{x} \end{pmatrix}, \begin{pmatrix} 0 & 0 & 0 \\ 0 & \mathbf{x} & 0 \\ \mathbf{x} & 0 & 0 \end{pmatrix}, \begin{pmatrix} 0 & 0 & 0 \\ \mathbf{x} & 0 & 0 \\ 0 & 0 & 0 \end{pmatrix}, \begin{pmatrix} 0 & 0 & \mathbf{x} \\ 0 & 0 & 0 \\ 0 & 0 & 0 \end{pmatrix} \quad (4.13)$$

- The next set of constraints is derived from the fact that the phase matrices are not independent: Entries that correspond to Γ_1 and Δ_1 have to match the first Higgs charge and are therefore equal (up to a minus sign, due to the complex conjugation of $\tilde{\Phi}_1$, as defined in (2.88)). Same for the entries corresponding to Γ_2 and Δ_2 . Thus, there are two more equations that can be applied to the phase matrices:

$$\Theta_{\text{down}}|_{\text{combined text.}} = \begin{pmatrix} \frac{1}{2}d_3 - \frac{1}{2}u_2 & 2q_2 - \frac{1}{2}d_3 - \frac{3}{2}u_2 & q_2 - u_2 \\ -2q_2 + \frac{3}{2}d_3 + \frac{1}{2}u_2 & \frac{1}{2}d_3 - \frac{1}{2}u_2 & -q_2 + d_3 \\ -q_2 + d_3 & q_2 - u_2 & \frac{1}{2}d_3 - \frac{1}{2}u_2 \end{pmatrix} \quad (4.14)$$

$$\Theta_{\text{up}}|_{\text{combined text.}} = \begin{pmatrix} -\frac{1}{2}d_3 + \frac{1}{2}u_2 & q_2 - d_3 & 2q_2 - \frac{3}{2}d_3 - \frac{1}{2}u_2 \\ -2q_2 + \frac{1}{2}d_3 + \frac{3}{2}u_2 & -q_2 + u_2 & -\frac{1}{2}d_3 + \frac{1}{2}u_2 \\ -q_2 + u_2 & -\frac{1}{2}d_3 + \frac{1}{2}u_2 & q_2 - d_3 \end{pmatrix} \quad (4.15)$$

- As the next step, the anomaly equations come into play. Before solving them, the conditions derived from the textures are substituted into the expressions for the anomaly coefficients (4.2), which in this case yields

$$A_{331'} = 0 \quad A_{221'} = \frac{9}{2}(d_3 + u_2) \quad A_{111'} = -\frac{3}{4}(d_3 + 5u_2) \quad (4.16)$$

$$A_{11'1'} = \frac{3}{4}(d_3 - u_2)(5d_3 + 7u_2) \quad A_{1'1'1'} = -\frac{27}{4}(d_3 - u_2)(d_3^2 - u_2^3). \quad (4.17)$$

Please note that, for this very example, the $A_{331'}$ coefficient is already zero due to the texture constraints.

As explained in the beginning of this section, the anomaly equations are solved stepwise. Solving the linear equations (4.16) for vanishing coefficients yields

$$d_3 = u_2 = 0, \quad (4.18)$$

which imposes the phase matrices

$$\Theta_{\text{down}}|_{\text{comb. text.} + \text{linear anomalies}} = \begin{pmatrix} 0 & 2q_2 & q_2 \\ -2q_2 & 0 & -q_2 \\ -q_2 & q_2 & 0 \end{pmatrix} \quad (4.19)$$

$$\Theta_{\text{up}}|_{\text{comb. text.} + \text{linear anomalies}} = \begin{pmatrix} 0 & q_2 & 2q_2 \\ -2q_2 & -q_2 & 0 \\ -q_2 & 0 & q_2 \end{pmatrix}. \quad (4.20)$$

- As a final step, the quadratic and cubic anomaly equations (4.17) have to be solved. In this example, however, both coefficients vanish automatically (substitute (4.18) into (4.17)) and do not impose additional constraints. Consequently, the final phase matrices are given in (4.19) and (4.20) already.

The patterns formed by the equal entries are still given by (4.12) and (4.13), which means they contain the original Yukawa textures (4.7). Thus, it is a "good" model.

Example of a "bad" model: Consider a slightly different set of textures

$$\Gamma_1 : \begin{pmatrix} \mathbf{x} & 0 & 0 \\ 0 & \mathbf{x} & 0 \\ 0 & 0 & \mathbf{x} \end{pmatrix}, \quad \Gamma_2 : \begin{pmatrix} 0 & 0 & \mathbf{x} \\ 0 & 0 & 0 \\ 0 & \mathbf{x} & 0 \end{pmatrix}, \quad \Delta_1 : \begin{pmatrix} 0 & 0 & 0 \\ 0 & 0 & \mathbf{x} \\ 0 & \mathbf{x} & 0 \end{pmatrix}, \quad \Delta_2 : \begin{pmatrix} \mathbf{x} & 0 & 0 \\ 0 & \mathbf{x} & 0 \\ 0 & 0 & 0 \end{pmatrix}. \quad (4.21)$$

- Jumping straight to the phase matrices after imposing the constraints derived from the textures and the relations between the phase matrices, one finds:

$$\Theta_{\text{down}}|_{\text{combined text.}} = \begin{pmatrix} \frac{1}{2}d_3 - \frac{1}{2}u_2 & 2q_2 - \frac{1}{2}d_3 - \frac{3}{2}u_2 & q_2 - u_2 \\ -2q_2 + \frac{3}{2}d_3 + \frac{1}{2}u_2 & \frac{1}{2}d_3 - \frac{1}{2}u_2 & -q_2 + d_3 \\ -q_2 + d_3 & q_2 - u_2 & \frac{1}{2}d_3 - \frac{1}{2}u_2 \end{pmatrix} \quad (4.22)$$

$$\Theta_{\text{up}}|_{\text{combined text.}} = \begin{pmatrix} -\frac{1}{2}d_3 + \frac{1}{2}u_2 & q_2 - d_3 & 2q_2 - \frac{3}{2}d_3 - \frac{1}{2}u_2 \\ -2q_2 + \frac{1}{2}d_3 + \frac{3}{2}u_2 & -q_2 + u_2 & -\frac{1}{2}d_3 + \frac{1}{2}u_2 \\ -q_2 + u_2 & -\frac{1}{2}d_3 + \frac{1}{2}u_2 & q_2 - d_3 \end{pmatrix} \quad (4.23)$$

At this stage, the equal entry patterns of Θ_{down} are of course identical to (4.12). The patterns of Θ_{up} are given as:

$$\Theta_{\text{up}} : \begin{pmatrix} 0 & 0 & 0 \\ 0 & 0 & \mathbf{x} \\ 0 & \mathbf{x} & 0 \end{pmatrix}, \begin{pmatrix} \mathbf{x} & 0 & 0 \\ 0 & \mathbf{x} & 0 \\ 0 & 0 & 0 \end{pmatrix}, \begin{pmatrix} 0 & \mathbf{x} & 0 \\ 0 & 0 & 0 \\ 0 & 0 & \mathbf{x} \end{pmatrix}, \begin{pmatrix} 0 & 0 & 0 \\ \mathbf{x} & 0 & 0 \\ 0 & 0 & 0 \end{pmatrix}, \begin{pmatrix} 0 & 0 & 0 \\ 0 & 0 & 0 \\ \mathbf{x} & 0 & 0 \end{pmatrix}, \begin{pmatrix} 0 & 0 & \mathbf{x} \\ 0 & 0 & 0 \\ 0 & 0 & 0 \end{pmatrix} \quad (4.24)$$

- After substituting the constraints that follow from the textures (4.21) into the anomaly coefficients (4.2), the linear equations read

$$A_{331'} = q_2 - \frac{1}{2}(d_3 + u_2) \quad A_{221'} = \frac{9}{2}(d_3 + u_2) \quad A_{111'} = \frac{1}{12}(16q_2 - 53u_2 - 17d_3). \quad (4.25)$$

When solved for vanishing coefficients, one finds

$$q_2 = d_3 = u_2 = 0. \quad (4.26)$$

At this point already, the Yukawa textures are lost, since imposing (4.26) on the phase matrices yields

$$\Theta_{\text{down}}|_{\text{comb. text. + linear anomalies}} = \begin{pmatrix} 0 & 0 & 0 \\ 0 & 0 & 0 \\ 0 & 0 & 0 \end{pmatrix} \quad (4.27)$$

$$\Theta_{\text{up}}|_{\text{comb. text. + linear anomalies}} = \begin{pmatrix} 0 & 0 & 0 \\ 0 & 0 & 0 \\ 0 & 0 & 0 \end{pmatrix}. \quad (4.28)$$

Consequently, the non-linear anomaly equations do not even have to be checked and the model is classified "bad".

4.1.4 Categorisation of models via the number of different charges

The resulting models may be categorised by the number of different charges in the three generations of each particle type.²³ A priori, there are three cases (all equal, two different or all different) for q_i , d_i and u_i , respectively. This allows us to divide the models into 27 categories.

However, it turns out that not all categories are possible. In order to have invertible mass matrices, the combined textures of Γ_1 and Γ_2 have to contain at least one non-zero entry in every row *and* every column.²⁴ Same argument goes for Δ_1 and Δ_2 . Consequently, the phase matrices' entries which correspond to the two Higgs charges have to satisfy the same condition.

As we will demonstrate in the following, this forbids any category that contains a sector, where the left-handed charges are all equal and right-handed ones all different, or vice versa. Similar to the example in section 3.1.2, consider a case where again all left-handed charges are equal to some charge, denoted as q . This imposes the following structure on the phase matrix for the down sector:

$$\Theta_{\text{down}}|_{q_i=q} = \begin{pmatrix} -q + d_1 & -q + d_2 & -q + d_3 \\ -q + d_1 & -q + d_2 & -q + d_3 \\ -q + d_1 & -q + d_2 & -q + d_3 \end{pmatrix} \quad (4.29)$$

In this form, it is evident that the phase matrix splits into columns of equal entries. In case of three different right-handed down charges d_i , any assignment to the Higgs charges will correspond to only two of the three columns. In other words, at least two of the d_i have to be equal in order to find one entry in each column and each row that corresponds to either of the two Higgs doublets.

²³Different charges does not mean that they are independent. It might very well be that some charges are proportional to the same free parameter, but with different coefficients in front.

²⁴Requiring the mass matrix to be invertible is equivalent to the condition of a non-zero determinant in (3.22) and ensures that all quarks are massive.

A similar analysis can be done for the up sector, where the Θ_{down} would split into columns, instead. Furthermore, one may also exclude cases where either of the right-handed charges are all equal while there are three different left-handed charges. This is because it would lead to a splitting of one of the phase matrices into rows of equal values.

We checked carefully that neither of these four cases occurs in any of the 116 models. On top, we verified that all the remaining categories were covered (for a summary, see Table 3).

number of different charges		(d_R, u_R)								
		(1,1)	(1,2)	(1,3)	(2,1)	(2,2)	(2,3)	(3,1)	(3,2)	(3,3)
q_L	1	Grey	Grey	Dark	Grey	Grey	Dark	Dark	Dark	Dark
	2	Grey	Grey	Grey	Grey	Grey	Grey	Grey	Grey	Grey
	3	Dark	Dark	Dark	Dark	Grey	Grey	Dark	Grey	Grey

Table 3: Categorisation via number of different charges. Dark cells are forbidden, due to non-invertible mass matrices. Grey cells correspond to the categories covered by the textures in [9].

4.1.5 Invariance under permutations

Before presenting the results of our studies for the quark sector, it is necessary to discuss the independence of different models. In fact, many texture pairs are related by permutations of columns or rows or both. In this section, we will discuss the physical consequences and conclude, in which cases the related models may be considered equal.

When comparing models, the four down and up textures have to be treated as a whole. Any permutation from the left, i.e. any permutation of rows, has an impact on observables. However, permuting the q_L charges in the same way corresponds to a simple relabelling.

For example, consider a permutation of the first and second row in *all* Yukawa matrices of the "good" model (4.7), i.e.

$$\Gamma_1 = \begin{pmatrix} \mathbf{x} & 0 & 0 \\ 0 & \mathbf{x} & 0 \\ 0 & 0 & \mathbf{x} \end{pmatrix} \rightarrow \Gamma'_1 = \begin{pmatrix} 0 & \mathbf{x} & 0 \\ \mathbf{x} & 0 & 0 \\ 0 & 0 & \mathbf{x} \end{pmatrix}, \dots \quad (4.30)$$

This implies that the Yukawa Lagrangian (3.1) changes as²⁵

$$-\Gamma_1^{11} \bar{q}_L^1 \Phi_1 d_R^1 - \Gamma_1^{22} \bar{q}_L^2 \Phi_1 d_R^2 - \dots \rightarrow -\underbrace{\Gamma_1'^{21}}_{\cong \Gamma_1^{11}} \bar{q}_L^2 \Phi_1 d_R^1 - \underbrace{\Gamma_1'^{12}}_{\cong \Gamma_1^{22}} \bar{q}_L^1 \Phi_1 d_R^2 - \dots \quad (4.31)$$

²⁵Please note that no fixed values are assigned to the Yukawa entries in this discussion, which allows us to identify terms before and after the permutation.

It is evident that the Lagrangian is identical, if $q_1 = q'_2$ and $q_2 = q'_1$. This, however, corresponds to nothing but a permutation of the first and second left-handed charge in the original model.

Analogously, column permutations leave the Lagrangian invariant, if the right-handed charges are permuted in the same way. The difference is, however, that right-handed charges are singlets and therefore independent for down and up sector. This implies that one may perform different column permutations on the down sector than on the up sector. As long as the right-handed charges are permuted accordingly, the models are equal.

Throughout the remainder of this thesis, any "good" model is presented by its textures and the charges derived from the anomaly equations. If the numerical procedure led to a second model that - up to the permutations described above - featured identical textures and derived charges, the models were regarded as equal and are presented only once.

4.1.6 Possible models for the quark sector

For the quark sector, models that allow for anomaly cancellation cover only three of the 17 possible categories, as presented in Table 4. Remarkably, these models fall only into the categories with the same number of different charges for each of the three types of particles.

number of different charges		(d_R, u_R)								
		(1,1)	(1,2)	(1,3)	(2,1)	(2,2)	(2,3)	(3,1)	(3,2)	(3,3)
q_L	1	Q_1								
	2					Q_2				
	3									Q_3

Table 4: Categorisation of Table 3, highlighting the models that already allow for anomaly cancellation with quarks only (green cells).

The textures and charges that correspond to the highlighted categories are listed in the following. For a more compact notation, the charges are arranged in vectors denoted \vec{x}_p , where the label $p = q, d, u, \Phi$ corresponds to the charges q_i, d_i, u_i and φ_a , respectively.

Quarks only category Q_1 :

$$\begin{aligned}
\Gamma_1 : \begin{pmatrix} \mathbf{x} & \mathbf{x} & \mathbf{x} \\ \mathbf{x} & \mathbf{x} & \mathbf{x} \\ \mathbf{x} & \mathbf{x} & \mathbf{x} \end{pmatrix} & \quad \Gamma_2 : \begin{pmatrix} 0 & 0 & 0 \\ 0 & 0 & 0 \\ 0 & 0 & 0 \end{pmatrix} & \quad \Delta_1 : \begin{pmatrix} \mathbf{x} & \mathbf{x} & \mathbf{x} \\ \mathbf{x} & \mathbf{x} & \mathbf{x} \\ \mathbf{x} & \mathbf{x} & \mathbf{x} \end{pmatrix} & \quad \Delta_2 : \begin{pmatrix} 0 & 0 & 0 \\ 0 & 0 & 0 \\ 0 & 0 & 0 \end{pmatrix} & \quad (4.32) \\
\vec{x}_q = (0, 0, 0) & \quad \vec{x}_d = (0, 0, 0) & \quad \vec{x}_u = (0, 0, 0) & \quad \vec{x}_\Phi = (0, \text{free charge})
\end{aligned}$$

Please note that, in this model, the first Higgs doublet is SM like. All SM particle $U(1)'$ charges are zero and the only field that transforms is the added Higgs doublet. However, since it does not couple to the quark sector at all, it may take any charge under $U(1)'$. This model is usually referred to as the Inert Higgs Model or Inert Doublet Model [7],[27].

For the two remaining categories, the charges are proportional to one free parameter. Thus, this "free charge" may be absorbed into the definition of the coupling in g'_1 (3.24). Hence we present only the numerical factors in front.²⁶

Quarks only category Q_2 :

$$(i) \quad \Gamma_1 : \begin{pmatrix} \mathbf{x} & 0 & 0 \\ \mathbf{x} & 0 & 0 \\ 0 & 0 & 0 \end{pmatrix} \quad \Gamma_2 : \begin{pmatrix} 0 & \mathbf{x} & \mathbf{x} \\ 0 & \mathbf{x} & \mathbf{x} \\ \mathbf{x} & 0 & 0 \end{pmatrix} \quad \Delta_1 : \begin{pmatrix} 0 & 0 & 0 \\ 0 & 0 & 0 \\ \mathbf{x} & \mathbf{x} & 0 \end{pmatrix} \quad \Delta_2 : \begin{pmatrix} \mathbf{x} & \mathbf{x} & 0 \\ \mathbf{x} & \mathbf{x} & 0 \\ 0 & 0 & \mathbf{x} \end{pmatrix} \quad (4.33)$$

$$\vec{x}_q = (1, 1, -2) \quad \vec{x}_d = (-2, 1, 1) \quad \vec{x}_u = (1, 1, -2) \quad \vec{x}_\Phi = (3, 0)$$

$$(ii) \quad \Gamma_1 \leftrightarrow \Delta_2 \quad \text{and} \quad \Gamma_2 \leftrightarrow \Delta_1 \quad (4.34)$$

$$\vec{x}_q = (1, 1, -2) \quad \vec{x}_d = (1, 1, -2) \quad \vec{x}_u = (-2, 1, 1) \quad \vec{x}_\Phi = (0, -3)$$

Finally, the category with three different charges for each particle type.

Quarks only category Q_3 :

$$(i) \quad \Gamma_1 : \begin{pmatrix} \mathbf{x} & 0 & 0 \\ 0 & \mathbf{x} & 0 \\ 0 & 0 & \mathbf{x} \end{pmatrix} \quad \Gamma_2 : \begin{pmatrix} 0 & 0 & \mathbf{x} \\ 0 & 0 & 0 \\ 0 & \mathbf{x} & 0 \end{pmatrix} \quad \Delta_1 : \begin{pmatrix} \mathbf{x} & 0 & 0 \\ 0 & 0 & \mathbf{x} \\ 0 & \mathbf{x} & 0 \end{pmatrix} \quad \Delta_2 : \begin{pmatrix} 0 & 0 & 0 \\ 0 & \mathbf{x} & 0 \\ \mathbf{x} & 0 & 0 \end{pmatrix} \quad (4.35)$$

$$\vec{x}_q = (-1, 1, 0) \quad \vec{x}_d = (-1, 1, 0) \quad \vec{x}_u = (-1, 0, 1) \quad \vec{x}_\Phi = (0, -1)$$

$$(ii) \quad \Gamma_1 \leftrightarrow \Delta_2 \quad \text{and} \quad \Gamma_2 \leftrightarrow \Delta_1 \quad (4.36)$$

$$\vec{x}_q = (-1, 1, 0) \quad \vec{x}_d = (-1, 0, 1) \quad \vec{x}_u = (-1, 1, 0) \quad \vec{x}_\Phi = (1, 0)$$

As a general feature of the "quarks only" models, we see that in each of them all quark types share the same set of charges, up to permutations.

4.1.7 Origin of the zero Higgs charge and extension to the lepton sector

Another characteristic shared by the "quarks only" models (4.32) to (4.36) is that one of the Higgs charges is always zero. This can be understood in the following way:

In each of these models, there is at least one Yukawa matrix that features a diagonal of non-zero entries. For any entry on the diagonal, the corresponding Higgs charge φ_a has to cancel the difference between the left-handed quark charge q_i and the right-handed quark charge of the same family d_i or u_i , depending on the sector.

²⁶Please remember that we do not present all column and row permutations explicitly (see section 4.1.5).

As an example, consider model (4.35). The non-zero diagonal is featured in Γ_1 . The corresponding phases for each entry have to cancel, which implies the following three equations:

$$-q_i + d_i + \varphi_1 = 0 \quad \text{with } i = 1, 2, 3 \quad (4.37)$$

Adding the three equations yields

$$-\underbrace{\sum_{i=1}^3 q_i}_{=0} + \underbrace{\sum_{i=1}^3 d_i}_{=0} + 3\varphi_1 = 0 \quad \Rightarrow \quad \boxed{\varphi_1 = 0}, \quad (4.38)$$

where the first two anomaly equations from (4.2) were used.

A similar argument may be applied if the non-zero diagonal is featured in one of the other Yukawa matrices, including the up sector (see third equation in (4.2)). Thus, there is always one zero Higgs charge.

It is important to note that the zero Higgs charge is a direct consequence of the anomaly equations, while in [9] this was taken as an assumption. However, for our study of models with charged leptons in section 4.2, we will see that, in general, both Higgs charges are non-zero.

As a final remark for this section, it needs to be emphasized that the zero Higgs charge is what allows for a trivial extension of these models to the lepton sector. In fact, the leptons can be added by allowing SM like couplings to the Higgs doublet with zero charge and forbidding any couplings to the other one. In doing so, the leptons keep the zero charges under $U(1)'$ that were imposed in the beginning of section 4.1, so everything is consistent.

Consequently, the models presented in (4.32) to (4.36) are not limited to quarks only but may serve as models for the full particle content.

4.2 Quarks and charged leptons

In this section, we repeat the studies of section 4.1, but without the restriction to the quark sector. Instead, the full particle content, as presented in Table 2, is considered.²⁷ Thus, the relevant Yukawa Lagrangian is given in (3.1).

²⁷Please note that we do not include right-handed neutrinos for this analysis.

4.2.1 Anomaly equations for quarks and charged leptons

Starting from the anomaly coefficients (3.28) and (3.29), one may derive a set of six independent anomaly equations:

$$\left. \begin{array}{l} 0 \stackrel{!}{=} A_{331'} \\ 0 \stackrel{!}{=} A_{221'} \\ 0 \stackrel{!}{=} A_{111'} \\ 0 \stackrel{!}{=} A_{gg1'} \\ 0 \stackrel{!}{=} A_{11'1'} \\ 0 \stackrel{!}{=} A_{1'1'1'} \end{array} \right\} \Leftrightarrow \left\{ \begin{array}{l} \sum_{i=1}^3 l_i \stackrel{!}{=} -3 \sum_{i=1}^3 q_i \\ \sum_{i=1}^3 d_i \stackrel{!}{=} -2 \sum_{i=1}^3 q_i \\ \sum_{i=1}^3 u_i \stackrel{!}{=} +4 \sum_{i=1}^3 q_i \\ \sum_{i=1}^3 e_i \stackrel{!}{=} -6 \sum_{i=1}^3 q_i \\ 0 \stackrel{!}{=} \sum_{i=1}^3 (q_i^2 - l_i^2 - 2u_i^2 + d_i^2 + e_i^2) \\ 0 \stackrel{!}{=} \sum_{i=1}^3 (6q_i^3 + 2l_i^3 - 3u_i^3 - 3d_i^3 - e_i^3) \end{array} \right. \quad (4.39)$$

Compared to the "quarks only" case (4.2), there are six additional parameters while the number of equations increased by only one. This implies more freedom for possible solutions and we expect to find more "good" models as a consequence.

4.2.2 Numerical procedure for quarks and charged leptons

The numerical procedure is highly similar to what was presented in sections 4.1.2 and 4.1.3, so we will present the shared methods fairly quickly focus on the supplementary technicalities, when considering the full particle content.

After extracting and imposing the constraints from the quark textures, the extended anomaly equations (4.39) are solved to provide up to six solutions. If any of these solutions keeps the original textures unspoiled, the model is classified as "interesting".

Due to their contribution the anomaly equations, the lepton charges l_i and e_i are constrained by the conditions that were derived from the quark sector. However, requesting sufficient couplings of the Higgs fields in the lepton sector imposes additional constraints, as we will discuss in the following.

In analogy to the phase matrices for down and up sector (3.16) and (3.17), we define a phase matrix for the lepton sector:

$$\Theta_{\text{lepton}} := \begin{pmatrix} -l_1 + e_1 & -l_1 + e_2 & -l_1 + e_3 \\ -l_2 + e_1 & -l_2 + e_2 & -l_2 + e_3 \\ -l_3 + e_1 & -l_3 + e_2 & -l_3 + e_3 \end{pmatrix} \quad (4.40)$$

Based on the discussion of section 4.1.2, it is evident that the equal entry patterns of the lepton phase matrix (4.40) provide the possible textures for the lepton Yukawa matrices Π_1 , Π_2 , as introduced in (3.1).

In accordance with the quark mass matrices (3.4), the lepton mass matrix after electroweak spontaneous symmetry breaking is given as

$$M_e = \frac{1}{\sqrt{2}}(v_1\Pi_1 + v_2\Pi_2). \quad (4.41)$$

Since all charged leptons are massive, this matrix has to be invertible. As discussed in section 4.1.4, this implies that the combined textures of Π_1 and Π_2 have to feature at least one entry in every column *and* every row. This is precisely the origin of the additional constraints we are about to derive.

In order to take the above condition into account, one has to impose a minimal combined texture of Π_1 and Π_2 . There are six possibilities, given as

$$\begin{pmatrix} \mathbf{x} & 0 & 0 \\ 0 & \mathbf{x} & 0 \\ 0 & 0 & \mathbf{x} \end{pmatrix}, \begin{pmatrix} \mathbf{x} & 0 & 0 \\ 0 & 0 & \mathbf{x} \\ 0 & \mathbf{x} & 0 \end{pmatrix}, \begin{pmatrix} 0 & \mathbf{x} & 0 \\ \mathbf{x} & 0 & 0 \\ 0 & 0 & \mathbf{x} \end{pmatrix}, \begin{pmatrix} 0 & \mathbf{x} & 0 \\ 0 & 0 & \mathbf{x} \\ \mathbf{x} & 0 & 0 \end{pmatrix}, \begin{pmatrix} 0 & 0 & \mathbf{x} \\ \mathbf{x} & 0 & 0 \\ 0 & \mathbf{x} & 0 \end{pmatrix}, \begin{pmatrix} 0 & 0 & \mathbf{x} \\ 0 & \mathbf{x} & 0 \\ \mathbf{x} & 0 & 0 \end{pmatrix}. \quad (4.42)$$

However, all these structures are related by permutations. In section 4.1.5, we discussed that all these texture permutations correspond to the same model, if the charges are permuted accordingly. Since permutations in the lepton sector are independent from permutations in the quark sector, we can choose one structure without the loss of generality. Thus, we have the freedom to impose the diagonal structure as the minimal combined texture.

This diagonal structure must be featured as a pattern in the lepton phase matrix (4.40), formed by entries corresponding to the two Higgs charges. This leads to four subclasses, given by:²⁸

$$-\Theta_{\text{lepton}} = \begin{pmatrix} \varphi_1 & & \\ & \varphi_1 & \\ & & \varphi_1 \end{pmatrix}, \begin{pmatrix} \varphi_1 & & \\ & \varphi_1 & \\ & & \varphi_2 \end{pmatrix}, \begin{pmatrix} \varphi_1 & & \\ & \varphi_2 & \\ & & \varphi_2 \end{pmatrix} \text{ or } \begin{pmatrix} \varphi_2 & & \\ & \varphi_2 & \\ & & \varphi_2 \end{pmatrix} \quad (4.43)$$

In accordance with (3.20), the minus sign on the left ensures cancellation of the overall phase of this entry. Please note that the off-diagonal entries are left empty, because there are no constraints on them (in fact, some of them might be equal to either of the Higgs charges, as well).

The numerical implementation was done in form of a loop: Each of the four subclasses provides three equations (three diagonal entries). These additional constraints were imposed separately on the "interesting" models, splitting each of these into four submodels.

²⁸There are priori eight subclasses, since each of the three diagonal entries may correspond to either of the two Higgs doublets. However, the four classes presented here are sufficient, since the remaining four correspond to permutations of the second and third case and are therefore equivalent.

Finally, the same criteria as in the "quarks only" case were applied (see section 4.1.3). If the original quark Yukawa textures were still present as equal entry patterns in the quark phase matrices *and* if the solutions allowed for fractional charges, a submodel was classified "good". Otherwise, the model was ruled out.

4.2.3 Possible models for quarks and charged leptons

In order to present the results for quarks and charged leptons, we will use again the categorisation via the number of different charges that was introduced in section 4.1.4.

It turns out that all the "good" models, found by the numerical procedure presented in the last section, feature three different lepton charges for l_i and e_i , respectively. Thus, it is convenient to list only the number of different quark charges, which corresponds to how we presented the "quarks only" models in Table 4. On this basis, find the "quarks and charged leptons" models that allow for anomaly cancellation categorised in Table 5, along with the "good" models for the quark sector that can be trivially extended to the lepton sector (see sections 4.1.6 and 4.1.7).²⁹

number of different charges		(d_R, u_R)								
		(1,1)	(1,2)	(1,3)	(2,1)	(2,2)	(2,3)	(3,1)	(3,2)	(3,3)
q_L	1	Q₁				L₁				
	2		L₂		L'₂	Q₂	L₃		L'₃	
	3					(L₄)	L₅		L'₅	Q₃

Table 5: Extension of Table 4 by the "quarks and charged leptons" models that allow for anomaly cancellation (blue cells). The latter feature always three different charges for l_i and e_i , respectively.

As opposed to the results from section 4.1.6, the charges of the newfound models are given in terms of not one but two parameters. However, in analogy to the "quarks only" case, one of these free charges may be absorbed into the coupling g'_1 (3.24). We chose to normalise the first left-handed quark charge, i.e. $q_1 = 1$. Consequently, the models here are presented with one free parameter, labelled as x .³⁰

Similar to the quark charges, the left- and right-handed lepton charges are arranged in

²⁹Because of the latter reason, the good "quarks only" textures were not studied again for the extended particle content. It is therefore interesting to note that no additional models were found within the categories, where all particle types feature the same number of different charges.

³⁰Please remember that we present the models up to column and row permutations (see section 4.1.5).

vectors denoted \vec{x}_1 and \vec{x}_e , respectively. With that being said, the anomaly-free models for the "quarks and charged leptons" case are given as:

Quarks and charged leptons category \mathbf{L}_1 : Two models with $\vec{x}_q = (1, 1, 1)$.

$$\begin{aligned}
& \Gamma_1 : \begin{pmatrix} \mathbf{x} & \mathbf{x} & 0 \\ \mathbf{x} & \mathbf{x} & 0 \\ \mathbf{x} & \mathbf{x} & 0 \end{pmatrix} \quad \Gamma_2 : \begin{pmatrix} 0 & 0 & \mathbf{x} \\ 0 & 0 & \mathbf{x} \\ 0 & 0 & \mathbf{x} \end{pmatrix} \quad \Delta_1 : \begin{pmatrix} 0 & \mathbf{x} & \mathbf{x} \\ 0 & \mathbf{x} & \mathbf{x} \\ 0 & \mathbf{x} & \mathbf{x} \end{pmatrix} \quad \Delta_2 : \begin{pmatrix} \mathbf{x} & 0 & 0 \\ \mathbf{x} & 0 & 0 \\ \mathbf{x} & 0 & 0 \end{pmatrix} \\
\text{(i)} \quad & \vec{x}_d = (2 - x, 2 - x, -10 + 2x) \quad \vec{x}_u = (12 - 2x, x, x) \\
& \vec{x}_1 = (1 - x, x - 7, -3) \quad \vec{x}_e = (2 - 2x, -6, 2x - 14) \\
& \vec{x}_\Phi = (x - 1, 11 - 2x)
\end{aligned} \tag{4.44}$$

$$\begin{aligned}
& \Gamma_1 \leftrightarrow \Delta_2 \quad \text{and} \quad \Gamma_2 \leftrightarrow \Delta_1 \\
\text{(ii)} \quad & \vec{x}_d = (-3 - 2x, x, x) \quad \vec{x}_u = (2 - x, 2 - x, 4 + 2x) \\
& \vec{x}_1 = (-5 - x, x - 1, -3) \quad \vec{x}_e = (-6, 2x - 2, -10 - 2x) \\
& \vec{x}_\Phi = (2x + 7, 1 - x)
\end{aligned} \tag{4.45}$$

The following two models show up as two different categories, but are in fact highly connected. Since they share the same set of textures and feature identical left-handed charges \vec{x}_q , we present them together.

Quarks and charged leptons category \mathbf{L}_2 : $\vec{x}_q = (1, 1, -\frac{3}{2}x - 2)$

$$\begin{aligned}
& \Gamma_1 : \begin{pmatrix} \mathbf{x} & \mathbf{x} & \mathbf{x} \\ \mathbf{x} & \mathbf{x} & \mathbf{x} \\ 0 & 0 & 0 \end{pmatrix} \quad \Gamma_2 : \begin{pmatrix} 0 & 0 & 0 \\ 0 & 0 & 0 \\ \mathbf{x} & \mathbf{x} & \mathbf{x} \end{pmatrix} \quad \Delta_1 : \begin{pmatrix} \mathbf{x} & \mathbf{x} & 0 \\ \mathbf{x} & \mathbf{x} & 0 \\ 0 & 0 & 0 \end{pmatrix} \quad \Delta_2 : \begin{pmatrix} 0 & 0 & 0 \\ 0 & 0 & 0 \\ 0 & 0 & \mathbf{x} \end{pmatrix} \\
\text{(i)} \quad & \vec{x}_d = (x, x, x) \quad \vec{x}_u = (2 - x, 2 - x, -4 - 4x) \\
& \vec{x}_1 = (x - 1, -5 - x, 6 + \frac{9}{2}x) \quad \vec{x}_e = (2x - 2, -6, 7x + 8) \\
& \vec{x}_\Phi = (1 - x, -2 - \frac{5}{2}x)
\end{aligned} \tag{4.46}$$

Quarks and charged leptons category \mathbf{L}'_2 : $\vec{x}_q = (1, 1, -\frac{3}{2}x - 2)$

$$\begin{aligned}
& \Gamma_1 \leftrightarrow \Delta_2 \quad \text{and} \quad \Gamma_2 \leftrightarrow \Delta_1 \\
\text{(ii)} \quad & \vec{x}_d = (2 + 2x, 2 + 2x, -4 - x) \quad \vec{x}_u = (-2x, -2x, -2x) \\
& \vec{x}_1 = (1 + 2x, -7 - 2x, \frac{9}{2}x + 6) \quad \vec{x}_e = (2 + 4x, -6, 4 + 5x) \\
& \vec{x}_\Phi = (2 - \frac{1}{2}x, -1 - 2x)
\end{aligned} \tag{4.47}$$

In as similar way, we present the connected categories \mathbf{L}_3 and \mathbf{L}'_3 .

Quarks and charged leptons category \mathbf{L}_3 : $\vec{x}_q = (1, 1, -\frac{1}{2} - \frac{3}{4}x)$

$$\begin{aligned}
& \Gamma_1 : \begin{pmatrix} \mathbf{x} & \mathbf{x} & 0 \\ \mathbf{x} & \mathbf{x} & 0 \\ 0 & 0 & 0 \end{pmatrix} \quad \Gamma_2 : \begin{pmatrix} 0 & 0 & \mathbf{x} \\ 0 & 0 & \mathbf{x} \\ \mathbf{x} & \mathbf{x} & 0 \end{pmatrix} \quad \Delta_1 : \begin{pmatrix} 0 & \mathbf{x} & 0 \\ 0 & \mathbf{x} & 0 \\ \mathbf{x} & 0 & 0 \end{pmatrix} \quad \Delta_2 : \begin{pmatrix} \mathbf{x} & 0 & 0 \\ \mathbf{x} & 0 & 0 \\ 0 & 0 & \mathbf{x} \end{pmatrix} \\
\text{(i)} \quad & \vec{x}_d = \left(\frac{1}{4}x - \frac{3}{2}, \frac{1}{4}x - \frac{3}{2}, x \right) \quad \vec{x}_u = \left(2 - x, \frac{7}{2} - \frac{1}{4}x, \frac{1}{2} - \frac{7}{4}x \right) \\
& \vec{x}_1 = \left(x - 1, \frac{5}{4}x - \frac{1}{2}, -3 \right) \quad \vec{x}_e = \left(2x - 2, \frac{9}{4}x - \frac{3}{2}, \frac{1}{4}x - \frac{11}{2} \right) \\
& \vec{x}_\Phi = \left(\frac{5}{2} - \frac{1}{4}x, 1 - x \right)
\end{aligned} \tag{4.48}$$

Quarks and charged leptons category \mathbf{L}'_3 : $\vec{x}_q = (1, 1, -\frac{1}{2} - \frac{3}{4}x)$

$$\begin{aligned}
& \Gamma_1 \leftrightarrow \Delta_2 \quad \text{and} \quad \Gamma_2 \leftrightarrow \Delta_1 \\
\text{(ii)} \quad & \vec{x}_d = \left(\frac{1}{2}x - 1, \frac{1}{2} + \frac{5}{4}x, -\frac{5}{2} - \frac{1}{4}x \right) \quad \vec{x}_u = \left(\frac{3}{2} - \frac{5}{4}x, \frac{3}{2} - \frac{5}{4}x, 3 - \frac{1}{2}x \right) \\
& \vec{x}_1 = \left(\frac{1}{2} + \frac{7}{4}x, -2 + \frac{1}{2}x, -3 \right) \quad \vec{x}_e = \left(\frac{9}{4}x - \frac{3}{2}, x - 4, \frac{5}{4}x - \frac{7}{2} \right) \\
& \vec{x}_\Phi = \left(2 - \frac{1}{2}x, \frac{1}{2} - \frac{5}{4}x \right)
\end{aligned} \tag{4.49}$$

The following two models of category \mathbf{L}_4 were classified "good" in our scan.

Quarks and charged leptons category \mathbf{L}_4 : $\vec{x}_q = (1, -\frac{1}{5} - \frac{3}{5}x, \frac{2}{5} - \frac{3}{10}x)$

$$\begin{aligned}
& \Gamma_1 : \begin{pmatrix} 0 & 0 & 0 \\ 0 & 0 & 0 \\ \mathbf{x} & \mathbf{x} & 0 \end{pmatrix} \quad \Gamma_2 : \begin{pmatrix} \mathbf{x} & \mathbf{x} & 0 \\ 0 & 0 & \mathbf{x} \\ 0 & 0 & 0 \end{pmatrix} \quad \Delta_1 : \begin{pmatrix} 0 & 0 & 0 \\ 0 & 0 & 0 \\ \mathbf{x} & \mathbf{x} & 0 \end{pmatrix} \quad \Delta_2 : \begin{pmatrix} 0 & 0 & \mathbf{x} \\ \mathbf{x} & \mathbf{x} & 0 \\ 0 & 0 & 0 \end{pmatrix} \\
\text{(i)} \quad & \vec{x}_d = \left(\frac{4}{5}x - \frac{2}{5}, \frac{4}{5}x - \frac{2}{5}, \frac{1}{5}x - \frac{8}{5} \right) \quad \vec{x}_u = \left(\frac{6}{5} - \frac{7}{5}x, \frac{6}{5} - \frac{7}{5}x, \frac{12}{5} - \frac{4}{5}x \right) \\
& \vec{x}_1 = \left(x - 1, \frac{4}{5}x - \frac{7}{5}, \frac{9}{10}x - \frac{6}{5} \right) \quad \vec{x}_e = \left(\frac{9}{5}x - \frac{12}{5}, \frac{8}{5}x - \frac{14}{7}, 2x - 2 \right) \\
& \vec{x}_\Phi = \left(\frac{4}{5} - \frac{11}{10}x, \frac{7}{5} - \frac{4}{5}x \right)
\end{aligned} \tag{4.50}$$

$$\begin{aligned}
& \Gamma_1 \leftrightarrow \Delta_2 \quad \text{and} \quad \Gamma_2 \leftrightarrow \Delta_1 \\
\text{(ii)} \quad & \vec{x}_d = \left(-\frac{3}{5} + \frac{2}{5}x, -\frac{3}{5} + \frac{2}{5}x, x \right) \quad \vec{x}_u = \left(2 - x, 2 - x, \frac{4}{5} - \frac{8}{5}x \right) \\
& \vec{x}_1 = \left(-\frac{7}{5} + \frac{4}{5}x, x - 1, -\frac{6}{5} + \frac{9}{10}x \right) \quad \vec{x}_e = \left(-\frac{12}{5} + \frac{9}{5}x, 2x - 2, -\frac{14}{5} + \frac{8}{5}x \right) \\
& \vec{x}_\Phi = \left(1 - x, \frac{8}{5} - \frac{7}{10}x \right)
\end{aligned} \tag{4.51}$$

However, a closer look reveals that both quark mass matrices, as defined in (3.4), feature a block-diagonal structure. In fact, the non-zero entries form the patterns

$$M_d|_{\mathbf{L}_4} = \begin{pmatrix} \mathbf{x} & \mathbf{x} & 0 \\ 0 & 0 & \mathbf{x} \\ \mathbf{x} & \mathbf{x} & 0 \end{pmatrix} \quad \text{and} \quad M_u|_{\mathbf{L}_4} = \begin{pmatrix} 0 & 0 & \mathbf{x} \\ \mathbf{x} & \mathbf{x} & 0 \\ \mathbf{x} & \mathbf{x} & 0 \end{pmatrix}, \quad (4.52)$$

which leads to block-diagonal Hermitian combinations H_d (3.7) and H_u (3.8):³¹

$$H_d|_{\mathbf{L}_4} = \begin{pmatrix} \mathbf{x} & 0 & \mathbf{x} \\ 0 & \mathbf{x} & 0 \\ \mathbf{x} & 0 & \mathbf{x} \end{pmatrix} \quad \text{and} \quad H_u|_{\mathbf{L}_4} = \begin{pmatrix} \mathbf{x} & 0 & 0 \\ 0 & \mathbf{x} & \mathbf{x} \\ 0 & \mathbf{x} & \mathbf{x} \end{pmatrix} \quad (4.53)$$

At this point, one can argue that a block-diagonal structure in both Hermitian matrices, like in (4.53), will lead to unitary diagonalising matrices that are parametrised by only one phase each. As a result, the CKM matrix (3.12) will be parametrised by only two angles. However, the general unitary CKM matrix is parametrised by three angles (and the CP phase) [28], so the textures are not sufficient.

A similar analysis can be done for case (ii) in category \mathbf{L}_4 . Consequently, both models do not provide sufficient quark mixing and are therefore unphysical.

The final two connected categories are given as:

Quarks and charged leptons category \mathbf{L}_5 : $\vec{x}_q = (1, -2 - \frac{3}{2}x, -\frac{1}{2} - \frac{3}{4}x)$

$$\begin{aligned} \Gamma_1 : \begin{pmatrix} 0 & 0 & 0 \\ 0 & 0 & \mathbf{x} \\ \mathbf{x} & \mathbf{x} & 0 \end{pmatrix} \quad \Gamma_2 : \begin{pmatrix} \mathbf{x} & \mathbf{x} & 0 \\ 0 & 0 & 0 \\ 0 & 0 & \mathbf{x} \end{pmatrix} \quad \Delta_1 : \begin{pmatrix} 0 & 0 & 0 \\ 0 & 0 & \mathbf{x} \\ 0 & \mathbf{x} & 0 \end{pmatrix} \quad \Delta_2 : \begin{pmatrix} \mathbf{x} & 0 & 0 \\ 0 & \mathbf{x} & 0 \\ 0 & 0 & 0 \end{pmatrix} \\ \text{(i)} \quad \vec{x}_d = \left(\frac{3}{2} + \frac{7}{4}x, \frac{3}{2} + \frac{7}{4}x, x \right) \quad \vec{x}_u = \left(\frac{1}{2} - \frac{7}{4}x, -\frac{5}{2} - \frac{13}{4}x, -4 - 4x \right) \\ \vec{x}_l = \left(\frac{11}{2} + \frac{17}{4}x, 2 + \frac{5}{2}x, -3 \right) \quad \vec{x}_e = \left(\frac{15}{2} + \frac{27}{4}x, 4 + 5x, -\frac{5}{2} + \frac{7}{4}x \right) \\ \vec{x}_\Phi = \left(-2 - \frac{5}{2}x, -\frac{1}{2} - \frac{7}{4}x \right) \end{aligned} \quad (4.54)$$

Quarks and charged leptons category \mathbf{L}'_5 : $\vec{x}_q = (1, -2 - \frac{3}{2}x, -\frac{1}{2} - \frac{3}{4}x)$

$$\begin{aligned} \Gamma_1 \leftrightarrow \Delta_2 \quad \text{and} \quad \Gamma_2 \leftrightarrow \Delta_1 \\ \text{(ii)} \quad \vec{x}_d = \left(\frac{7}{2} + \frac{11}{4}x, \frac{1}{2} + \frac{5}{4}x, \frac{1}{2}x - 1 \right) \quad \vec{x}_u = \left(-\frac{3}{2} - \frac{11}{4}x, -\frac{3}{2} - \frac{11}{4}x, -3 - \frac{7}{2}x \right) \\ \vec{x}_l = \left(\frac{13}{2} + \frac{19}{4}x, 2x + 1, -3 \right) \quad \vec{x}_e = \left(\frac{15}{2} + \frac{27}{4}x, 2 + 4x, \frac{11}{4}x - \frac{1}{2} \right) \\ \vec{x}_\Phi = \left(-\frac{5}{2} - \frac{11}{4}x, -1 - 2x \right) \end{aligned} \quad (4.55)$$

³¹As before, \mathbf{x} denotes a general complex entry.

5 Reproducing the CKM matrix for an example model

In this section, we will study one of the "good" models in more detail and investigate its ability to provide a CKM matrix that matches the experimental values. For this purpose, we chose the model presented in category \mathbf{Q}_3 (4.35), because, out of the "quarks only" models, it features the least amount of non-zero Yukawa entries.³² This means that it has the least amount of free parameters and hence should be the easiest to solve.

As mentioned in section 3.1, it is convenient to work with the Hermitian matrices H_d (3.7) and H_u (3.8), rather than attempting to find the mass matrices M_d and M_u (3.4), directly. Due to their Hermiticity, they feature three invariants under diagonalisation, namely

$$\text{Tr}(H_f) \equiv \text{Tr}(D_f^2) = m_1^2 + m_2^2 + m_3^2 \quad (5.1)$$

$$\det H_f \equiv \det D_f^2 = m_1^2 m_2^2 m_3^2 \quad (5.2)$$

$$\frac{(\text{Tr} H_f)^2 - \text{Tr}(H_f^2)}{2} \equiv \frac{(\text{Tr} D_f^2)^2 - \text{Tr}(D_f^4)}{2} = m_1^2 m_2^2 + m_2^2 m_3^2 + m_1^2 m_3^2, \quad (5.3)$$

where the quark masses are given as $(m_1, m_2, m_3) = (m_{d/u}, m_{s/c}, m_{b/t})$ for the label $f = d/u$, respectively.

5.1 Down sector

The textures given in (4.35) impose the general structure of the mass matrix for the down sector

$$M_d = \begin{pmatrix} z_1 & 0 & z_2 \\ 0 & z_3 & 0 \\ 0 & z_4 & z_5 \end{pmatrix} \quad \text{with complex numbers} \quad z_j = r_j e^{i\alpha_j}, \quad (5.4)$$

where the Einstein summation convention does not apply for the latter equation. The phases α_j can be removed via two diagonal matrices, by defining

$$M'_d := \begin{pmatrix} e^{i\beta_1} & & \\ & e^{i\beta_2} & \\ & & e^{i\beta_3} \end{pmatrix} M_d \begin{pmatrix} e^{i\gamma_1} & & \\ & e^{i\gamma_2} & \\ & & e^{i\gamma_3} \end{pmatrix} \quad (5.5)$$

$$= \begin{pmatrix} r_1 e^{i(\alpha_1 + \beta_1 + \gamma_1)} & 0 & r_2 e^{i(\alpha_5 + \beta_1 + \gamma_3)} \\ 0 & r_3 e^{i(\alpha_2 + \beta_2 + \gamma_2)} & 0 \\ 0 & r_4 e^{i(\alpha_4 + \beta_3 + \gamma_2)} & r_5 e^{i(\alpha_3 + \beta_3 + \gamma_3)} \end{pmatrix}. \quad (5.6)$$

It is evident that the six parameters $\beta_{1/2/3}$ and $\gamma_{1/2/3}$ can be chosen in such a way that they cancel the five different phases $\alpha_{1/2/3/4/5}$, yielding

$$M'_d = \begin{pmatrix} r_1 & 0 & r_2 \\ 0 & r_3 & 0 \\ 0 & r_4 & r_5 \end{pmatrix} \quad \text{with real numbers} \quad r_j > 0, \forall j. \quad (5.7)$$

³²Together with model (4.36), of course.

Please note that removing the phases in this way is consistent, as long as one redefines the bi-diagonalising matrices (3.5) as

$$V'_{\text{dL}}{}^\dagger M'_d V'_{\text{dR}} = V_{\text{dL}}{}^\dagger M_d V_{\text{dR}} = D_d, \quad (5.8)$$

which, by making use of (5.5), implies³³

$$V'_{\text{dL}} := \begin{pmatrix} e^{i\beta_1} & & \\ & e^{i\beta_2} & \\ & & e^{i\beta_3} \end{pmatrix} V_{\text{dL}} \quad \text{and} \quad V'_{\text{dR}} := \begin{pmatrix} e^{-i\gamma_1} & & \\ & e^{-i\gamma_2} & \\ & & e^{-i\gamma_3} \end{pmatrix} V_{\text{dR}}. \quad (5.9)$$

In accordance with (3.7), one may define the Hermitian matrix $H'_d = M'_d M_d{}^\dagger$. Using (5.7), it can be seen that it features the following invariants under diagonalisation:

$$\text{Tr} H'_d = r_1^2 + r_2^2 + r_3^2 + r_4^2 + r_5^2 \quad (5.10)$$

$$\det H'_d = r_1^2 r_3^2 r_5^2 \quad (5.11)$$

$$\frac{(\text{Tr} H'_d)^2 - \text{Tr}(H_d'^2)}{2} = r_1^2 r_3^2 + r_1^2 r_4^2 + r_1^2 r_5^2 + r_2^2 r_3^2 + r_2^2 r_4^2 + r_3^2 r_5^2 \quad (5.12)$$

Combining (5.1) to (5.3) and (5.10) to (5.12), yields a set of three equations:

$$m_d^2 + m_s^2 + m_b^2 = r_1^2 + r_2^2 + r_3^2 + r_4^2 + r_5^2 \quad (5.13)$$

$$m_d^2 m_s^2 m_b^2 = r_1^2 r_3^2 r_5^2 \quad (5.14)$$

$$m_d^2 m_s^2 + m_s^2 m_b^2 + m_d^2 m_b^2 = r_1^2 r_3^2 + r_1^2 r_4^2 + r_1^2 r_5^2 + r_2^2 r_3^2 + r_2^2 r_4^2 + r_3^2 r_5^2 \quad (5.15)$$

This allows one to express three of the r_j in terms of the other two and the down-type quark masses, for instance:

$$\begin{aligned} r_2(r_1, r_3, m_d, m_s, m_b) &= \frac{1}{\sqrt{2}} \sqrt{A \pm \sqrt{A^2 + 4m_b^2 \left(\frac{m_d^2}{r_1^2} - 1 \right) (m_s^2 - r_1^2)(1 - \varepsilon_{r1})}} \\ r_4(r_1, r_3, m_d, m_s, m_b) &= \frac{1}{\sqrt{2}} \sqrt{B \mp \sqrt{A^2 + 4m_b^2 \left(\frac{m_d^2}{r_1^2} - 1 \right) (m_s^2 - r_1^2)(1 - \varepsilon_{r1})}} \\ r_5(r_1, r_3, m_d, m_s, m_b) &= \frac{m_d m_s m_b}{r_1 r_3}, \end{aligned} \quad (5.16)$$

where

$$A = m_3^2 \left(1 - \frac{m_d^2 m_s^2}{r_1^2 r_3^2} + \varepsilon_d + \varepsilon_s - 2\varepsilon_{r1} \right) \quad (5.17)$$

$$B = m_3^2 \left(1 - \frac{m_d^2 m_s^2}{r_1^2 r_3^2} + \varepsilon_d + \varepsilon_s - 2\varepsilon_{r3} \right) \quad (5.18)$$

$$\varepsilon_d = \frac{m_d^2}{m_b^2} \quad \varepsilon_s = \frac{m_s^2}{m_b^2} \quad \varepsilon_{r1} = \frac{r_1^2}{m_b^2} \quad \varepsilon_{r3} = \frac{r_3^2}{m_b^2}. \quad (5.19)$$

³³In general, this re-phasing is *not* consistent, because it has an impact on the (complex) CP phase inside the CKM matrix. However, in the end of this section, we will only be interested in the absolute values of all entries.

Since the quark masses are known from experiment, the above equations allow one to reduce the number of free parameters for M'_d to only two. Thus, we may conclude:

$$\boxed{M'_d = M'_d(r_1, r_3)} \quad (5.20)$$

5.2 Up sector

After removing the phases in the same way as for the down sector, we find the mass matrix

$$M'_u = \begin{pmatrix} s_1 & 0 & 0 \\ 0 & s_2 & s_3 \\ s_4 & s_5 & 0 \end{pmatrix} \quad \text{with real numbers } s_j > 0, \forall j. \quad (5.21)$$

The Hermitian matrix $H'_u = M'_u M'^{\dagger}_u$ features the following invariants under diagonalisation:

$$\text{Tr} H'_u = s_1^2 + s_2^2 + s_3^2 + s_4^2 + s_5^2 \quad (5.22)$$

$$\det H'_u = s_1^2 s_3^2 s_5^2 \quad (5.23)$$

$$\frac{(\text{Tr} H'_u)^2 - \text{Tr}(H'^2_u)}{2} = s_1^2 s_2^2 + s_1^2 s_3^2 + s_1^2 s_5^2 + s_2^2 s_4^2 + s_3^2 s_4^2 + s_3^2 s_5^2 \quad (5.24)$$

Using (5.1) to (5.3) and (5.22) to (5.24), one may again express three of the s_j in terms of the other two and the up-type quark masses, for instance:

$$\begin{aligned} s_2(s_1, s_3, m_u, m_c, m_t) &= \frac{1}{\sqrt{2}} \sqrt{C \pm \sqrt{C^2 + 4m_t^2 \left(\frac{m_u^2}{s_3^2} - 1 \right) (m_c^2 - s_3^2)(1 - \xi_{s3})}} \\ s_4(s_1, s_3, m_u, m_c, m_t) &= \frac{1}{\sqrt{2}} \sqrt{D \mp \sqrt{C^2 + 4m_t^2 \left(\frac{m_u^2}{s_3^2} - 1 \right) (m_c^2 - s_3^2)(1 - \xi_{s3})}} \\ s_5(s_1, s_3, m_u, m_c, m_t) &= \frac{m_u m_c m_t}{s_1 s_3}, \end{aligned} \quad (5.25)$$

where

$$C = m_t^2 \left(1 - \frac{m_u^2 m_c^2}{s_1^2 s_3^2} + \xi_u + \xi_c - 2\xi_{s3} \right) \quad (5.26)$$

$$D = m_t^2 \left(1 - \frac{m_u^2 m_c^2}{s_1^2 s_3^2} + \xi_u + \xi_c - 2\xi_{s1} \right) \quad (5.27)$$

$$\xi_u = \frac{m_u^2}{m_t^2} \quad \xi_c = \frac{m_c^2}{m_t^2} \quad \xi_{s1} = \frac{s_1^2}{m_t^2} \quad \xi_{s3} = \frac{s_3^2}{m_t^2}. \quad (5.28)$$

In analogy to the down sector, there are only two free parameters remaining after substituting the experimental values of the quark masses. Hence, we can conclude:

$$\boxed{M'_u = M'_u(s_1, s_3)} \quad (5.29)$$

The above equation and the result from the down sector (5.20) imply that there is a total of four free parameters for the two mass matrices M'_d and M'_u . For each choice of $r_{1/3}$, $s_{1/3}$, the Hermitian combinations H'_d and H'_u are fully determined, hence are their diagonalising matrices V'_{dL} , V'_{uL} .

Consequently, the CKM matrix (3.12) is determined by the same four parameters:

$$V'_{\text{CKM}}(r_1, r_3, s_1, s_3) = V'_{uL}(s_1, s_3)V'_{dL}(r_1, r_3) \quad (5.30)$$

Please note that the above expression for the CKM matrix differs from the original definition (3.12) only by a re-phasing of the entries (see (5.9)). Thus, the absolute values are identical and provide a physical quantity that can be compared to the experimental data, as we will present in the next section.

5.3 Parameter regions for a good CKM matrix

Starting from the derived analytic expressions for the mass matrices (5.16) and (5.25), we extracted conditions for the parameters. This was done by imposing a clear mass hierarchy

$$m_d \ll m_s \ll m_b \quad \text{and} \quad m_u \ll m_c \ll m_t, \quad (5.31)$$

respectively, and requesting the arguments of all square roots to be positive. This yielded the upper limits

$$r_1 < m_s, \quad r_3 < m_b \quad \text{and} \quad s_1 < m_c, \quad s_3 < m_t. \quad (5.32)$$

For our study, we limited our attention to the subclass, where also $s_3 < m_c$. Setting up a parameter scan with these limits, revealed a promising parameter region at

$$\boxed{r_1 \sim m_d, \quad r_3 \sim m_s \quad \text{and} \quad s_1 < m_c, \quad s_3 < m_c.} \quad (5.33)$$

An example point we found is

$$\begin{aligned} r_1 &= 0.00328897 \text{ GeV} & r_3 &= 0.112908 \text{ GeV} \\ s_1 &= 0.249161 \text{ GeV} & s_3 &= 0.0263323 \text{ GeV}, \end{aligned} \quad (5.34)$$

which leads to a CKM matrix with the absolute values given as (see (5.30))

$$|V_{\text{CKM}}|_{\text{example}} \equiv |V'_{\text{CKM}}|_{\text{example}} \approx \begin{pmatrix} 0.97339 & 0.22914 & 0.00357 \\ 0.22906 & 0.97231 & 0.0462 \\ 0.00712 & 0.0458 & 0.99892 \end{pmatrix}, \quad (5.35)$$

where the following numerical values of the quark masses were used (taken from [28]):

$$\begin{aligned} m_d &= 0.0048 \text{ GeV} & m_s &= 0.095 \text{ GeV} & m_b &= 4.18 \text{ GeV} \\ m_u &= 0.0023 \text{ GeV} & m_c &= 1.275 \text{ GeV} & m_t &= 173.21 \text{ GeV} \end{aligned} \quad (5.36)$$

When compared to the experimental data

$$|V_{\text{CKM}}|_{\text{experiment}} \approx \begin{pmatrix} 0.97427 & 0.22536 & 0.00355 \\ 0.22522 & 0.97343 & 0.0414 \\ 0.00886 & 0.0405 & 0.99914 \end{pmatrix}, \quad (5.37)$$

we see that, besides the 31, 23 and 32 component which differ by almost 20 %, 13 % and 12% respectively, the values are within 2 % deviation.³⁴

We would like to end this section by emphasising that, for time reasons, we did not perform a full numerical study. However, the region presented in (5.33) seems promising enough to serve as a starting point for even better results with smaller deviations from the experimental data.

³⁴The experimental values are taken from [28].

6 Conclusion and outlook

Starting from the flavour-dependent Abelian symmetries in the 2HDM studied by [9], we investigated the option to handle the unobserved Goldstone bosons by promoting the continuous global symmetries to gauge symmetries. In order to do this, we scrutinised the derived Yukawa textures in the context of gauge anomalies and isolated the ones which allow for anomaly cancellation under the new gauge group.

This was done in two steps: First, we focussed our attention to the quark sector, where we derived three distinct categories of models that exhibit anomaly cancellation without the necessity to include leptons. The categorisation is based on the number of different charges for each particle type. Each of these models may be trivially extended by a lepton sector and is therefore adaptable to the full particle content.

Second, we extended our studies to include the lepton sector. Due to the additional degrees of freedom, this provided an extra of eight models, where quarks and leptons have to enter the anomalies in order to allow cancellation. In analogy to the first scan, these eight models could be divided into four distinct groups.

In summary, it can be said that imposing anomaly cancellation in the presented way reduced the number of models from initially 116 to 13 only (up to permutations). For each of these models, we presented the Yukawa textures and charges of all particles under the new gauge symmetry in detail, so they may be used for future studies.

Furthermore, we presented an in-depth study of one example model and demonstrated its ability to reproduce the absolute values of the CKM matrix within a maximum deviation of less than 20 % from the experimental data (significantly less in other entries). In our parameter scan, we discovered a promising region for the four model parameters. We consider it auspicious enough to provide even better results and to serve as a starting point for a full numerical study in the future.

Acknowledgements

First and foremost, I want to thank Hugo Serôdio, who turned out to be a great supervisor and without whom this thesis would not have been possible. Thank you for the numerous meetings, the patience when answering my (sometimes repetitive) questions and the overall guidance throughout the project.

Second, I want to express my gratitude to Roman Pasechnik, who provided the official supervision, always had an eye on me and contributed to the thesis as well as the entire project with valuable comments and discussions.

Third, I want to say "Thanks folks!" to my office mates: Thank you, Laurie, for helping me, whenever I struggled with English expressions and thank you for not forcing the American spelling on me. Thank you, Baptiste, for being a faithful companion throughout my time in Lund; thank you for the taco nights, the weekly workout, the endless conversations and your ability, to make even the longest office days enjoyable.

Last but definitely not least, I want to thank my family and my girlfriend who stood by my side and believed in me whenever I struggled. Thank you for your unconditional love, your emotional support and the nights we spent talking instead of sleeping. Thank you that you exist. I love you!

A Appendix

A.1 Pauli matrices and Gell-Mann matrices

Following the convention of [11], the Pauli matrices denoted as σ^j for $j = 1, 2, 3$ are given as

$$\sigma^1 = \begin{pmatrix} 0 & 1 \\ 1 & 0 \end{pmatrix} \quad \sigma^2 = \begin{pmatrix} 0 & -i \\ i & 0 \end{pmatrix} \quad \sigma^3 = \begin{pmatrix} 1 & 0 \\ 0 & -1 \end{pmatrix}. \quad (\text{A.1})$$

Correspondingly, the structure constants of the SU(2) generators (2.3) are equal to the three-dimensional Levi-Civita symbols

$$f^{jkl} = \varepsilon^{jkl} := \begin{cases} 1 & jkl = \text{even permutation of } 123 \\ -1 & jkl = \text{odd permutation of } 123 \\ 0 & \text{else.} \end{cases} \quad (\text{A.2})$$

The anticommutator of two Pauli matrices is given as

$$\{\sigma^j, \sigma^k\} = 2\delta^{jk}\mathbb{1}_2, \quad (\text{A.3})$$

where δ^{jk} denotes the Kronecker delta, defined as

$$\delta^{jk} := \begin{cases} 1 & j = k \\ 0 & j \neq k. \end{cases} \quad (\text{A.4})$$

The Gell-Mann matrices labelled λ^a for $a = 1, \dots, 8$ are given as:

$$\begin{aligned} \lambda^1 &= \begin{pmatrix} 0 & 1 & 0 \\ 1 & 0 & 0 \\ 0 & 0 & 0 \end{pmatrix} & \lambda^2 &= \begin{pmatrix} 0 & -i & 0 \\ i & 0 & 0 \\ 0 & 0 & 0 \end{pmatrix} & \lambda^3 &= \begin{pmatrix} 1 & 0 & 0 \\ 0 & -1 & 0 \\ 0 & 0 & 0 \end{pmatrix} & \lambda^4 &= \begin{pmatrix} 0 & 0 & 1 \\ 0 & 0 & 0 \\ 1 & 0 & 0 \end{pmatrix} \\ \lambda^5 &= \begin{pmatrix} 0 & 0 & -i \\ 0 & 0 & 0 \\ i & 0 & 0 \end{pmatrix} & \lambda^6 &= \begin{pmatrix} 0 & 0 & 0 \\ 0 & 0 & 1 \\ 0 & 1 & 0 \end{pmatrix} & \lambda^7 &= \begin{pmatrix} 0 & 0 & 0 \\ 0 & 0 & -i \\ 0 & i & 0 \end{pmatrix} & \lambda^8 &= \frac{1}{\sqrt{3}} \begin{pmatrix} 1 & 0 & 0 \\ 0 & 1 & 0 \\ 0 & 0 & -2 \end{pmatrix} \end{aligned} \quad (\text{A.5})$$

The corresponding structure constants for the SU(3) generators (2.3) are given by

$$f^{abc} = \begin{cases} f_{147} = -f_{156} = f_{246} = f_{257} = f_{345} = -f_{367} = \frac{1}{2} \\ f_{123} = 1 \\ f_{458} = f_{678} = \frac{\sqrt{3}}{2} \\ \text{zero otherwise.} \end{cases} \quad (\text{A.6})$$

A.2 Dirac matrices

The Dirac matrices γ^μ for $\mu = 0, 1, 2, 3$ and the additional γ^5 in Dirac-Pauli representation [3] are

$$\gamma^0 = \begin{pmatrix} \mathbb{1}_2 & 0 \\ 0 & -\mathbb{1}_2 \end{pmatrix} \quad \gamma^i = \begin{pmatrix} 0 & \sigma^i \\ -\sigma^i & 0 \end{pmatrix} \quad \gamma^5 \equiv i\gamma^0\gamma^1\gamma^2\gamma^3 = \begin{pmatrix} 0 & \mathbb{1}_2 \\ \mathbb{1}_2 & 0 \end{pmatrix}, \quad (\text{A.7})$$

where σ^i are the usual Pauli matrices. The Dirac matrices and γ^5 satisfy

$$\{\gamma^\mu, \gamma^\nu\} = 2g^{\mu\nu}\mathbb{1}_4 \quad \text{and} \quad \{\gamma^5, \gamma^\nu\} = 0, \quad (\text{A.8})$$

with the metric tensor given as

$$(g^{\mu\nu}) = \begin{pmatrix} 1 & 0 & 0 & 0 \\ 0 & -1 & 0 & 0 \\ 0 & 0 & -1 & 0 \\ 0 & 0 & 0 & -1 \end{pmatrix}. \quad (\text{A.9})$$

In addition, the Dirac matrices obey the following trace identity [29]

$$\begin{aligned} \text{Tr} \{ \gamma^5 \gamma^\mu \gamma^\nu \gamma^\lambda \gamma^\rho \gamma^\sigma \gamma^\tau \} = 4i & (g^{\mu\nu} \varepsilon^{\lambda\rho\sigma\tau} - g^{\mu\lambda} \varepsilon^{\nu\rho\sigma\tau} + g^{\nu\lambda} \varepsilon^{\mu\rho\sigma\tau} \\ & + g^{\rho\sigma} \varepsilon^{\mu\nu\lambda\tau} - g^{\rho\tau} \varepsilon^{\mu\nu\lambda\sigma} + g^{\sigma\tau} \varepsilon^{\mu\nu\lambda\rho}), \end{aligned} \quad (\text{A.10})$$

which reduces for $\gamma^\sigma \gamma^\tau = (\gamma^0)^2 = \mathbb{1}_4$ to

$$\text{Tr} \{ \gamma^5 \gamma^\mu \gamma^\nu \gamma^\lambda \gamma^\rho \} = 4i \varepsilon^{\mu\nu\lambda\rho}, \quad (\text{A.11})$$

with the four-dimensional Levi-Civita symbol

$$\varepsilon^{\mu\nu\rho\sigma} = \begin{cases} 1 & \mu\nu\rho\sigma = \text{even permutation of } 0123 \\ -1 & \mu\nu\rho\sigma = \text{odd permutation of } 0123 \\ 0 & \text{else.} \end{cases} \quad (\text{A.12})$$

A.3 Time ordering

Time ordering is denoted by the operator \mathcal{T} . One has to distinguish between products of bosonic and fermionic nature, due to the different (anti-)commutation relations [10]. In the bosonic case, we have

$$\mathcal{T}\phi_A(x)\phi_B(y) = \theta(x^0 - y^0)\phi_A(x)\phi_B(y) + \theta(y^0 - x^0)\phi_B(y)\phi_A(x), \quad (\text{A.13})$$

whilst in the fermionic case we find

$$\mathcal{T}\psi_A(x)\bar{\psi}_B(y) = \theta(x^0 - y^0)\psi_A(x)\bar{\psi}_B(y) - \theta(y^0 - x^0)\bar{\psi}_B(y)\psi_A(x), \quad (\text{A.14})$$

with the Heaviside step function $\theta(x) = \begin{cases} 0 & x \leq 0 \\ 1 & x > 0. \end{cases}$

A.4 Shifting linear divergent integrals in Minkowski space

Consider a shift in the integration variable $x \rightarrow x + a$ of linear divergent integral in n dimensions

$$\Delta_n(a) = \int d^n x (f(x+a) - f(x)) \quad (\text{A.15})$$

$$= \int d^n x (a^\mu \partial_\mu f(x) + a^\mu a^\nu \partial_\mu \partial_\nu f(x) + \dots). \quad (\text{A.16})$$

Applying the Gauss theorem yields [11]

$$\Delta_n(a) = a^\mu \lim_{R \rightarrow \infty} \frac{R_\mu}{R} S^{n-1}(R) f(R), \quad (\text{A.17})$$

with $S^{n-1}(R)$ denoting the surface of an $(n-1)$ -dimensional sphere with radius R . In four dimensions, we have $S^3(R) = 2\pi^2 R^3$. Thus, we find

$$\Delta_4(a) = 2\pi^2 a^\mu \lim_{R \rightarrow \infty} R_\mu R^2 f(R). \quad (\text{A.18})$$

Careful, this is the result for 4D Euclidean space. However, it can be turned into the Minkowskian case via $x^4 = ix^0$ [21], which means an overall factor i has to be added. Consequently one finds

$$\Delta_{\text{Minkowski}}(a) = i2\pi^2 a^\mu \lim_{R \rightarrow \infty} R_\mu R^2 f(R). \quad (\text{A.19})$$

A.5 Feynman slash identities

In order to derive the anomalous axial Ward identity, the following slash identity is used:

$$\not{q}\gamma^5 = \gamma^5(\not{p} - \not{q} - m) + (\not{p} - m)\gamma^5 + 2m\gamma^5 \quad (\text{A.20})$$

The following two identities are used in the derivation of the anomalous vector Ward identities:

$$\begin{aligned} \not{k}_1 \frac{1}{\not{p} - m} &= 1 - (\not{p} - \not{k}_1 - m) \frac{1}{\not{p} - m} \\ \frac{1}{\not{p} - \not{q} - m} \not{k}_1 &= -1 + \frac{1}{\not{p} - \not{q} - m} (\not{p} - \not{k}_2 - m) \end{aligned} \quad (\text{A.21})$$

A.6 Trivial anomaly cancellation

Consider two simple non-Abelian groups G and G' with traceless generators

$$\text{Tr}(T_G^a) \equiv 0 \quad \text{and} \quad \text{Tr}(T_{G'}^a) \equiv 0 \quad (\text{A.22})$$

and the Abelian group $U(1)$ with the generator $T_{U(1)}$. They form a semisimple symmetry group $G \times G' \times U(1)$ with three types of generators:

$$\tilde{T}_G^a := T_G^a \otimes \mathbb{1}_{G'} \otimes \mathbb{1}_{U(1)} \quad (\text{A.23})$$

$$\tilde{T}_{G'}^a := \mathbb{1}_G \otimes T_{G'}^a \otimes \mathbb{1}_{U(1)} \quad (\text{A.24})$$

$$\tilde{T}_{U(1)}^a \equiv \tilde{T}_{U(1)} := \mathbb{1}_G \otimes \mathbb{1}_{G'} \otimes T_{U(1)} \quad (\text{A.25})$$

Keeping in mind that $\text{Tr}(A \otimes B) = \text{Tr}(A)\text{Tr}(B)$, one finds

$$\begin{aligned} G^2 \times G' &\propto \sum_{\text{d.o.f.}} \text{Tr} \left(\left\{ \tilde{T}_G^a, \tilde{T}_G^b \right\} \tilde{T}_{G'}^c \right) = \\ &= \sum_{\text{d.o.f.}} \text{Tr} \left(\left\{ T_G^a, T_G^b \right\} \otimes T_{G'}^c \otimes \mathbb{1}_{U(1)} \right) = \\ &= \sum_{\text{d.o.f.}} \text{Tr} \left(\left\{ T_G^a, T_G^b \right\} \right) \underbrace{\text{Tr}(T_{G'}^c)}_{\equiv 0} \text{Tr}(\mathbb{1}_{U(1)}) \equiv 0, \end{aligned} \quad (\text{A.26})$$

$$\begin{aligned} G \times G' \times U(1) &\propto \sum_{\text{d.o.f.}} \text{Tr} \left(\left\{ \tilde{T}_G^a, \tilde{T}_{G'}^b \right\} \tilde{T}_{U(1)}^c \right) = \\ &= 2 \sum_{\text{d.o.f.}} \text{Tr} \left(T_G^a \otimes T_{G'}^b \otimes T_{U(1)} \right) = \\ &= 2 \sum_{\text{d.o.f.}} \underbrace{\text{Tr}(T_G^a)}_{\equiv 0} \underbrace{\text{Tr}(T_{G'}^b)}_{\equiv 0} \text{Tr}(T_{U(1)}) \equiv 0 \end{aligned} \quad (\text{A.27})$$

$$\begin{aligned} \text{and } G \times [U(1)]^2 &\propto \sum_{\text{d.o.f.}} \text{Tr} \left(\left\{ \tilde{T}_{U(1)}^a, \tilde{T}_{U(1)}^b \right\} \tilde{T}_G^c \right) = \\ &= \sum_{\text{d.o.f.}} \text{Tr} \left(T_G^c \otimes \mathbb{1}_{G'} \otimes \{T_{U(1)}, T_{U(1)}\} \right) = \\ &= \sum_{\text{d.o.f.}} \underbrace{\text{Tr}(T_G^c)}_{\equiv 0} \text{Tr}(\mathbb{1}_{G'}) \text{Tr}(\{T_{U(1)}, T_{U(1)}\}) \equiv 0. \end{aligned} \quad (\text{A.28})$$

A.7 Goldstone's theorem

The Goldstone's theorem states that any spontaneously broken continuous global symmetry gives rise to a massless boson, usually referred to as Goldstone boson.

Following the proof of [10], consider a general Lagrangian

$$\mathcal{L} = \text{terms with derivatives} - V(\{\phi^a\}), \quad (\text{A.29})$$

with fields $\phi^a(x)$. Each field can take a constant value ϕ_0^a that minimises the potential, so

$$\left. \frac{\partial V}{\partial \phi^a} \right|_{\phi^a(x)=\phi_0^a} = 0. \quad (\text{A.30})$$

Taylor expansion around the minimum yields

$$V(\{\phi^a\}) = V(\{\phi_0^a\}) + \underbrace{\left. \frac{\partial V}{\partial \phi^a} \right|_{\phi_0^a}}_{=0} (\phi^a - \phi_0^a) + \frac{1}{2} \underbrace{\left. \frac{\partial^2 V}{\partial \phi^a \partial \phi^b} \right|_{\phi_0^a, \phi_0^b}}_{=m_{ab}^2} (\phi^a - \phi_0^a)(\phi^b - \phi_0^b), \quad (\text{A.31})$$

where the eigenvalues of m_{ab}^2 correspond to the masses of the fields. They are all positive, because $V(\{\phi_0^a\})$ is a minimum. Consider further a continuous symmetry transformation in its infinitesimal form $\phi^a \rightarrow \phi^a + \varepsilon \Delta \phi^a$ with the infinitesimal parameter ε . In the special case of only constant fields, the derivatives in (A.29) vanish, so the potential itself has to be invariant under the transformation. This means that

$$V(\phi^a) \stackrel{!}{=} V(\phi^a + \varepsilon \Delta \phi^a) \quad \Leftrightarrow \quad \Delta \phi^a \left. \frac{\partial V}{\partial \phi^a} \right|_{\phi_0^a} \stackrel{!}{=} 0. \quad (\text{A.32})$$

Taking the derivative with respect to ϕ^b and replacing the fields $\{\phi^a\}$ by their constant values $\{\phi_0^a\}$ yields

$$0 = \frac{\partial \Delta \phi^a}{\partial \phi^b} \underbrace{\left. \frac{\partial V}{\partial \phi^a} \right|_{\{\phi_0^a\}}}_{=0} + \Delta \phi^a \underbrace{\left. \frac{\partial^2 V}{\partial \phi^a \partial \phi^b} \right|_{\{\phi_0^a\}}}_{m_{ab}^2} \quad (\text{A.33})$$

Because the symmetry is spontaneously broken by the ground state, $\Delta \phi^a|_{\{\phi_0^a\}} \neq 0$ has to be an eigenvector of m_{ab}^2 with eigenvalue zero, which corresponds to a massless particle.

References

- [1] ATLAS Collaboration, G. Aad *et al.*, “Observation of a new particle in the search for the Standard Model Higgs boson with the ATLAS detector at the LHC,” *Phys. Lett.* **B716** (2012) 1–29, arXiv:1207.7214 [hep-ex].
- [2] CMS Collaboration, S. Chatrchyan *et al.*, “Observation of a new boson at a mass of 125 GeV with the CMS experiment at the LHC,” *Phys. Lett.* **B716** (2012) 30–61, arXiv:1207.7235 [hep-ex].
- [3] M. Thomson, *Modern particle physics*. Cambridge University Press, New York, 2013. <http://www-spires.fnal.gov/spires/find/books/www?cl=QC793.2.T46::2013>.
- [4] A. Dobado, A. Gomez-Nicola, A. L. Maroto, and J. R. Pelaez, *Effective lagrangians for the standard model*. 1997. <http://www-spires.fnal.gov/spires/find/books/www?cl=QC794.6.S75E34::1997>.
- [5] Z.-z. Xing, “Quark Mass Hierarchy and Flavor Mixing Puzzles,” *Int. J. Mod. Phys.* **A29** (2014) 1430067, arXiv:1411.2713 [hep-ph].
- [6] I. P. Ivanov, “Building and testing models with extended Higgs sectors,” arXiv:1702.03776 [hep-ph].
- [7] G. C. Branco, P. M. Ferreira, L. Lavoura, M. N. Rebelo, M. Sher, and J. P. Silva, “Theory and phenomenology of two-Higgs-doublet models,” *Phys. Rept.* **516** (2012) 1–102, arXiv:1106.0034 [hep-ph].
- [8] E. Noether, “Invariant Variation Problems,” *Gott. Nachr.* **1918** (1918) 235–257, arXiv:physics/0503066 [physics].
- [9] P. M. Ferreira and J. P. Silva, “Abelian symmetries in the two-Higgs-doublet model with fermions,” *Phys. Rev.* **D83** (2011) 065026, arXiv:1012.2874 [hep-ph].
- [10] M. E. Peskin and D. V. Schroeder, *An Introduction to quantum field theory*. 1995. <http://www-spires.fnal.gov/spires/find/books/www?cl=QC174.45.P465::1995>.
- [11] R. A. Bertlmann, *Anomalies in quantum field theory*. 1996. <http://www-spires.fnal.gov/spires/find/books/www?cl=QC174.45.B42::1996>.
- [12] M. Schwartz, “Lecture notes: IV-1: Yang-Mills theory.” <http://isites.harvard.edu/fs/docs/icb.topic1146666.files/IV-1-YangMills.pdf>, 2013. [accessed 30-January-2017].

- [13] S. Abel, “Lecture notes: Anomalies.” http://www.maths.dur.ac.uk/~dma0saa/lecture_notes.pdf, n.y. [accessed 16-January-2017].
- [14] S. B. Treiman, E. Witten, R. Jackiw, and B. Zumino, *CURRENT ALGEBRA AND ANOMALIES*. 1986. <http://www-spines.fnal.gov/spines/find/books/www?cl=QC793.3.A4C936::1985>.
- [15] R. E. Marshak, *Conceptual foundations of modern particle physics*. 1993. <http://www-spines.fnal.gov/spines/find/books/www?cl=QC793.2.M375::1993>.
- [16] S. L. Adler, “Axial vector vertex in spinor electrodynamics,” *Phys. Rev.* **177** (1969) 2426–2438.
- [17] J. S. Bell and R. Jackiw, “A PCAC puzzle: $\pi^0 \rightarrow \gamma \gamma$ in the sigma model,” *Nuovo Cim.* **A60** (1969) 47–61.
- [18] P. van Nieuwenhuizen, *Anomalies in quantum field theory: Cancellation of anomalies in $d = 10$ supergravity*, vol. B3 of *Leuven notes in mathematical and theoretical physics*. Leuven Univ. Pr., Leuven, Belgium, 1989.
- [19] J. Steinberger, “On the Use of subtraction fields and the lifetimes of some types of meson decay,” *Phys. Rev.* **76** (1949) 1180–1186.
- [20] J. Bijnens, A. Bramon, and F. Cornet, “Pseudoscalar Decays Into Photon-photon in Chiral Perturbation Theory,” *Phys. Rev. Lett.* **61** (1988) 1453.
- [21] A. Bilal, “Lectures on Anomalies,” [arXiv:0802.0634](https://arxiv.org/abs/0802.0634) [hep-th].
- [22] J. Horejsi, *Introduction to electroweak unification: Standard model from tree unitarity*. 1993. <http://lss.fnal.gov/archive/other/prs-hep-93-8.pdf>.
- [23] C. Campagnari and M. Franklin, “The Discovery of the top quark,” *Rev. Mod. Phys.* **69** (1997) 137–212, [arXiv:hep-ex/9608003](https://arxiv.org/abs/hep-ex/9608003) [hep-ex].
- [24] G. C. Branco, L. Lavoura, and J. P. Silva, *CP Violation*. Clarendon Press: Oxford, 1999. <http://www-spines.fnal.gov/spines/find/books/www?cl=QC793.3.V5B73::1999>.
- [25] J. Zinn-Justin, “Quantum field theory and critical phenomena,” *Int. Ser. Monogr. Phys.* **113** (2002) 1–1054.
- [26] H.-M. Chan and S. T. Tsou, “Some elementary gauge theory concepts,” *World Sci. Lect. Notes Phys.* **47** (1993) 1–156.
- [27] M. Krawczyk, N. Darvishi, and D. Sokolowska, “The Inert Doublet Model and its extensions,” *Acta Phys. Polon.* **B47** (2016) 183, [arXiv:1512.06437](https://arxiv.org/abs/1512.06437) [hep-ph].

- [28] **Particle Data Group** Collaboration, K. A. Olive *et al.*, “Review of Particle Physics,” *Chin. Phys.* **C38** (2014) 090001.
- [29] V. I. Borodulin, R. N. Rogalyov, and S. R. Slabospitskii, “CORE 3.1 (COmpendium of RElations, Version 3.1),” [arXiv:1702.08246](https://arxiv.org/abs/1702.08246) [hep-ph].